Genome-wide characterization and expression analysis of aquaporins in salt cress (*Eutrema salsugineum*)

Weiguo Qian, Xiaomin Yang, Jiawen Li, Rui Luo, Xiufeng Yan and Qiuying Pang

Alkali Soil Natural Environmental Science Center, Northeast Forestry University/Key Laboratory of Saline-alkali Vegetation Ecology Restoration in Oil Field, Ministry of Education, Harbin, China

ABSTRACT

Aquaporins (AQPs) serve as water channel proteins and belong to major intrinsic proteins (MIPs) family, functioning in rapidly and selectively transporting water and other small solutes across biological membranes. Importantly, AQPs have been shown to play a critical role in abiotic stress response pathways of plants. As a species closely related to *Arabidopsis thaliana*, *Eutrema salsugineum* has been proposed as a model for studying salt resistance in plants. Here we surveyed 35 full-length *AQP* genes in *E. salsugineum*, which could be grouped into four subfamilies including 12 plasma membrane intrinsic proteins (PIPs), 11 tonoplast intrinsic proteins (TIPs), nine NOD-like intrinsic proteins (NIPs), and three small basic intrinsic proteins (SIPs) by phylogenetic analysis. EsAQPs were comprised of 237–323 amino acids, with a theoretical molecular weight (MW) of 24.31–31.80 kDa and an isoelectric point (pI) value of 4.73–10.49. Functional prediction based on the NPA motif, aromatic/arginine (ar/R) selectivity filter, Froger's position and specificity-determining position suggested quite differences in substrate specificities of EsAQPs. *EsAQP*s exhibited global expressions in all organs as shown by gene expression profiles and should be play important roles in response to salt, cold and drought stresses. This study provides comprehensive bioinformation on AQPs in *E. salsugineum*, which would be helpful for gene function analysis for further studies.

Submitted 2 March 2019
Accepted 13 August 2019
Published 12 September 2019

Corresponding author
Qiuying Pang, qiuying@nefu.edu.cn

Academic editor
Francisco Balao

Additional Information and Declarations can be found on page 21

DOI **10.7717/peerj.7664**

Subjects Bioinformatics, Genomics, Plant Science
Keywords *Eutrema salsugineum*, Aquaporin, Abiotic stress, Gene structure, Expression pattern

INTRODUCTION

Water is the most abundant molecule in living cells, forming the basic medium in which all biochemical reactions take place (*Dev & Herbert, 2018*). Aquaporins (AQPs) belong to the major intrinsic proteins (MIPs) superfamily, which could selectively transport water molecules across the cell membrane. In addition, AQPs can also transport many small molecules, such as glycerol, urea, carbon dioxide (CO_2), silicon, boron, ammonia (NH_3) and hydrogen peroxide (H_2O_2) (*Biela et al., 1999*; *Gerbeau et al., 1999*; *Uehlein et al., 2003*; *Ma et al., 2006*; *Takano et al., 2006*; *Loqué et al., 2005*; *Dynowski et al., 2008*). AQP was first discovered in animals and subsequently found in almost all living organisms (*Gomes et al., 2009*). Compare to animals, plants have more robust and diverse AQPs. For instance, there are 35 AQPs in *Arabidopsis thaliana*, 33 in *Oryza sativa*, 40 in *Sorghum bicolor*, 72 in *Glycine*

max, 47 in *Cicer arietinum* and 45 in *Manihot esculenta* (*Johanson et al., 2001*; *Sakurai et al., 2005*; *Kadam et al., 2017*; *Zhang et al., 2013*; *Deokar & Tar'an, 2016*; *Putpeerawit et al., 2017*).

Plant AQPs can be divided into seven subfamilies based on the protein sequence similarity analysis. Plasma membrane intrinsic proteins (PIPs) are the largest subfamily of plant AQPs. The most of the PIPs are commonly localized in the plasma membrane and are further divided into two phylogenetic groups PIP1 and PIP2. Tonoplast intrinsic proteins (TIPs) subfamily is usually localized in the tonoplast, which contain five classes TIP1, TIP2, TIP3, TIP4 and TIP5. NOD26-like intrinsic proteins (NIPs) named from NIP protein (Nodulin-26, GmNOD26), were discovered in the plasma membrane of soybean cells (*Fortin, Morrison & Verma, 1987*). Small basic intrinsic proteins (SIPs) are typically localized in the endoplasmic reticulum. X intrinsic proteins (XIPs) are present in some dicots but absent in Brassicaceae and monocots (*Maurel et al., 2015*). GlpF-like intrinsic proteins (GIPs) are found in moss (*Physcomitrella patens*) and similar to bacterial glycerol channels (*Danielson & Johanson, 2008*; *Gustavsson et al., 2005*). Hybrid intrinsic proteins (HIPs) are found in fern (*Selaginella moellendorffii*) and moss (*Physcomitrella patens*, *Anderberg, Kjellbom & Johanson, 2012*; *Gustavsson et al., 2005*). Therefore, some classes (such as XIPs, HIPs, or GIPs) are considered to be lost during the evolution of certain plant lineages due to function redundancies (*Maurel et al., 2015*).

AQPs are highly conserved in molecular structure, consisting of six transmembrane α-helical domains (TM1-TM6) linked by five loops (A-E), with both the N and C terminal having a cytoplasmic orientation. There are two highly conserved NPA (Asn-Pro-Ala) motifs in two half helices (HB and HE) of loopB and loopE at the center of the pore that have substrate selectivity (*Taji et al., 2002*). The narrow aromatic/arginine (ar/R) selectivity filter is formed with four residues from TM helix 2 (H2), TM helix 5 (H5), and loop E (LE1 and LE2), which has been shown to provide a size barrier for solute permeability (*Bansal & Sankararamakrishnan, 2007*). Froger's position consists of five residues (P1-P5) that could transport two different types of molecules, water and glycerol (*Froger et al., 1998*). Moreover, it has been predicted that AQPs have nine specificity-determining positions (SDPs) for non-aqua substrates, such as ammonia, boron, carbon dioxide, hydrogen peroxide, silicon and urea, for each unique group (*Hove & Bhave, 2011*).

Salt cress previously named as *Thellungiella halophila* or *Thellungiella salsuginea* recently was corrected to *Eutrema salsugineum* based on taxonomy and systematics, which is a relative close to *A. thaliana* (*Koch & German, 2013*). As a salt-sensitive plant, *Arabidopsis* has certain limits to study the mechanism of salt and drought resistance. In contrast, *E. salsugineum*, with a small genome, is quite tolerant to salt, drought and low temperature stresses, being considered to be a halophyte model plant for investigating the mechanism of plant resistance to stress (*Zhu, 2001*; *Inan et al., 2004*). The *E. salsugineum* AQPs like TsTIP1;2, TsMIP6 and TsPIP1;1 have been found to play an important role in plant response to abiotic stress (*Wang et al., 2014*; *Sun et al., 2015*; *Li et al., 2018*). The *E. salsugineum* genome was sequenced in 2012 and 2013 at the chromosome level and scaffold level, respectively (*Wu et al., 2012*; *Yang et al., 2013*), promoting the bioinformatics analysis of whole aquaporin family.

In this study, a genome-wide analysis of *AQP* genes was carried out in *E. salsugineum*, a total of 35 full-length *AQP* genes were identified. Based on the phylogenetic analysis, we found that the identified EsAQPs were quite similar to AtAQPs. The EsAQPs could be grouped into four subfamilies, including PIPs, TIPs, NIPs and SIPs. Protein sequences, chromosome distributions, gene structures and putative functions were analyzed for each of these members. The expression level of *EsAQP* genes in different organs and the abundance change of *EsAQP* genes in response to salt, drought and cold stresses were also investigated.

MATERIALS & METHODS

Identification and chromosomal location of EsAQPs

The whole genome of *E. salsugineum* was downloaded from NCBI (https://www.ncbi.nlm.nih.gov/genome/12266, *Wu et al., 2012*; *Yang et al., 2013*). To identify *E. salsugineum AQP* candidate genes, a Hidden Markov Model (HMM) analysis was used. HMM profile of MIP (PF00230) was downloaded from Pfam protein family database (http://pfam.sanger.ac.uk/) and used as the query ($P < 0.05$) to search for AQP proteins in the *E. salsugineum* genome. To avoid missing potential AQP members, the NCBI BLAST tool was used to search *E. salaugineum* AQPs and known *Arabidopsis* AQP protein sequences as a query, and the top five aligned sequences were considered as candidates. After removing all of the redundant sequences, the sequences of putative *EsAQP* genes were loaded on relative chromosomes of *E. salsugineum* using the SnapGene tool. The map of the chromosome position of each *EsAQP* genes was drawn by MapInspect 1.0.

Classification, phylogenetic analysis and structural features

Multiple sequence alignments of putative AQP proteins were performed by ClustalW, and a phylogenetic tree was constructed using neighbor joining with MEGA 6.0 (*Tamura et al., 2013*). The transmembrane regions were detected using TOPCONS (http://topcons.cbr.su.se/pred/) and TMHMM (http://www.cbs.dtu.dk/services/TMHMM/). Protein subcellular localization of *E. salsugineum* AQPs was predicted in Plant-mPLoc (http://www.csbio.sjtu.edu.cn/bioinf/plant-multi/) and WoLF PSORT (http://www.genscript.com/wolf-psort.html). Functional predictions, such as NPA motifs, ar/R filters (H2, H5, LE1 and LE2), Froger's positions (P1-P5) and nine specificity-determining positions (SDP1-SDP9), were analyzed by the alignments with function known AQPs (*Quigley et al., 2001*; *Park et al., 2010*; *Hove & Bhave, 2011*). The gene structure for each *EsAQP* was illustrated with the Gene Structure Display Server 2.0 (http://gsds.cbi.pku.edu.cn/). The conserved motifs of EsAQP proteins were analyzed by MEME suite (http://meme-suite.org/).

Plant materials and stress treatments

E. salsugineum seeds (ecotype Shandong, China) were provided by Prof. Hui Zhang (Shandong Normal University, Jinan, China). The seeds were plated on 1/2 MS medium and treated at 4 °C in dark for 7 days, then cultured in plant growth chamber with illumination of 150 μmol/m^2/s, photoperiod 16/8 h of light/darkness at 25 °C and 60%

relative humidity. After one week, the seedlings were transferred into a mixed medium with soil and vermiculite (3:1). Vernalization treatment for bolting was conducted in 4-week old seedlings at 4 °C for 4 weeks, and then they were moved back to the growth chamber until they grew flowers. Samples of roots, stems, leaves, flowers and siliques were collected, immediately frozen in liquid nitrogen and stored at −80 °C for further analysis.

For abiotic stress assays, the 4-week old seedlings were exposed to 300 mM NaCl for 24 h as a salt stress condition, treated at 4 °C for 24 h as cold stress, and not irrigated until the soil moisture content was less than 20% for 7 days as drought stress. The aerial part of seedling was collected for further analysis.

RNA extraction, cDNA synthesis and qRT-PCR

The total RNA was extracted using TRIzol reagent (Takara) following the manufacturer's protocol. The quality of the RNA was determined using an ultraviolet spectrophotometer (BioMate 3S; Thermo Fisher). After removing genomic DNA contamination with DNase I, cDNA was synthesized by using the PrimeScript^{TM} RT Reagent Kit (Takara). Three biological replicates of cDNA samples were used for qRT-PCR analysis with three technical replicates.

Primers of EsPIP genes were designed using Primer 3.0 (http://bioinfo.ut.ee/primer3-0.4.0/) and the reference gene was taken from *Wang et al. (2014)*. All of primers were listed in Table S1. The qRT-PCR analysis was conducted in Applied Biosystems 7500 Real-Time PCR System (ABI, USA) by using SYBR Premix Ex TaqTM II (Takara). Reaction system contained 10 μl SYBR Premix Ex Taq II, 2 μl 5-fold diluted cDNA, 0.8 μl of each primer (10 mM), and ddH_2O to a final volume of 20 μl. The PCR program was set as follows: 95 °C for 30 s, followed by 40 cycles of 95 °C for 5 s and 60 °C for 34 s. Then, a melting curve was generated to analyze the specificity of each primer with a temperature shift from 60 to 95 °C. The fold changes of the *EsAQP* genes expression under abiotic stresses were calculated with the $2^{-\Delta\Delta}$Ct method, while the gene expressions level of *EsAQP* genes in each organ were calculated with the $^{\Delta}$Ct method. The heat map of gene expression pattern was visualized using HemI software.

Subcellular localization of EsPIP1;2 and EsPIP2;1 proteins

The coding sequences of EsPIP1;2 and EsPIP2;1 were amplified using primers containing the XbaI/SalI restriction site (Table S2). The purified products were subcloned into a reconstructed pBI121 vector which was composed of the XbaI/SalI site, and GFP. pBI121-EsPIP1;2-GFP and pBI121-EsPIP2;1-GFP vectors were transformed into *A. tumefaciens* strain GV3101. Then transient transformation in onion epidermis according to the method of *Xu et al. (2014)* took place. Images of epidermal cells were taken by fluorescence microscope with a mirror unit (U-BW).

Xenopus oocyte expression and osmotic water permeability assay

The coding regions of EsPIP1;2 and EsPIP2;1 were subcloned into pCS107 vector using the restriction sites BamHI and EcoRI (see primers in Table S2). After linearization, the cRNAs were synthesized *in vitro* using the Sp6 mMessage mMachine kit (Ambion). Oocyte preparation, injection, and expression were performed as described by *Hu et*

al. (2012) with a little modification. A total of 10 nl water or cRNAs of EsPIP1;2 and EsPIP2;1 (one ng/nl) were injected into oocytes, respectively, and then the oocytes were incubated at 18 °C for 48 h in Oocyte Culture Medium (OCM, 50% L-15, 40% HEPES (pH 7.4), 10% calf serum, 0.5% penicillin and 10 mg/ml streptomycin).The osmotic water permeability coefficient of oocytes was determined as described by *Zhang & Verkman (1991)*. To measure the osmotic water permeability coefficient, oocytes were transferred to 5-fold diluted OCM solution. Changes in the oocytes volume were monitored at room temperature with a microscope video system. Oocytes volumes (Vs) were calculated from the measured area of each oocyte. The osmotic Pf was calculated for the Erst 10 min using the formula $Pf = V_0[d(V/V_0)/dt]/[S_0 \times Vw\ (Osmin–Osmout)]$. V_0 and S_0 are the initial volume and surface area of each individual oocyte, respectively; $d(V/V_0)/dt$ is the relative volume increase per unit time; Vw is the molar volume of water (18 $cm^3\ mol^{-1}$); and Osmin–Osmout is the osmotic gradient between the inside and outside of the oocyte.

RESULTS

Characterization, classification and chromosome localization of EsAQPs

To extensively identify AQPs in *E. salsguineum*, HMM profile of the MIP domain (PF00230) was used. As a result, a total of 35 putative EsAQPs were identified for further analysis (Table 1). To classify the AQP members, a phylogenetic tree was constructed according to the similarity of AQP protein sequences in *E. salsugineum* and *Arabidopsis* through the neighbor-joining method (Fig. 1). Based on the phylogenetic analysis, we found that the identified EsAQPs have very high similarity with AtAQPs which can be grouped into four subfamilies, including 12 PIPs, 11 TIPs, nine NIPs and three SIPs. In addition, the EsPIP subfamily was further divided into two classes (five EsPIP1s and seven EsPIP2s), the EsTIP subfamily into five classes (three EsTIP1s, four EsTIP2s, two EsTIP3s, one EsTIP4s and one EsTIP5s), the EsNIP subfamily into seven classes (1 EsNIP1s, 1 EsNIP2s, 1 EsNIP3s, three EsNIP4s, one EsNIP5s, one EsNIP6s and one EsNIP7s), and the EsSIP subfamily into two classes (two EsSIP1s and one EsSIP2s). The nomenclature of *E. salsugineum* AQPs was based on their phylogenetic relationship with AtAQPs (Fig. 1). These results were also supported by the existing annotation for *E. salsugineum* obtained from Phytozyme (https://phytozome.jgi.doe.gov/pz/portal.html#!bulk?org=Org_Esalsugineum), most of our identified EsAQPs were matched to the existing annotations (Table S3). In addition, we have updated some annotations i.e., Thhalv10008397m and Thhalv10025910m, which were both annotated as PIP1;4 in Phytozyme, were renamed with EsPIP1;3 and EsPIP1;5, respectively, and other details were listed in Table S3. Compare to AtAQPs, PIP2;8 and NIP1;1 were missing in *E. salsugineum.* And TIP2;4 and NIP4;3 were identified in *E.salsugineum*, but not found in *Arabidopsis*, which were shared high similarity with their homologous genes. In *Arabidopsis*, 35 *AQP* genes were unevenly distributed on the five chromosomes *Feng et al. (2017)*. As shown in Table 1 and Fig. 2, the chromosomal locations of 34 *EsAQP* genes were randomly assigned to all the seven chromosomes. However, chromosomal location of *EsTIP2;2* could not be determined. Overall, AQPs from *E. salsugineum* had a very close relationship with those from *Arabidopsis.*

Table 1 Details of EsAQP genes identified from the genome-wide search analysis.

Name	Chromosomal Localization	Scaffold	Coding sequence	Protein ID	Plant-mPLoc	WoLF PSORT	Plant species	Subcellular localization	Reference
EsPIP1;1	Chr5;748,014~746,287	NW_006256838.1	XM_006402419.1	XP_006402482.1	plas	plas	*Oryza ativa*	plas	*Liu et al. (2013)*
EsPIP1;2	Chr4;24,198,933~24,200,732	NW_006256812.1	XM_006397718.1	XP_006397781.1	plas	plas	*Musa nana*	plas	*Sreedharan, Shekhawat & Ganapathi (2013)*
EsPIP1;3	Chr1;227,418~229,068	NW_006256612.1	XM_006418376.1	XP_006418439.1	plas	plas			
EsPIP1;4	Chr6;182,520~180,408	NW_006256756.1	XM_006396178.1	XP_006396241.1	plas	plas	*Arabidopsis thaliana*	plas	*Li et al. (2015)*
EsPIP1;5	Chr7;21,955,256~21,956,964	NW_006256909.1	XM_006413496.1	XP_006413559.1	plas	plas			
EsPIP2;1	Chr5;3,815,044~3,817,131	NW_006256858.1	XM_006403628.1	XP_006403691.1	plas	plas	*A. thaliana*	plas	*Li et al. (2011)*
EsPIP2;2	Chr4;20,408,518~20,407,373	NW_006256908.1	XM_006410833.1	XP_006410896.1	plas	plas	*Vitis vinifera*	plas	*Leitão et al. (2012)*
EsPIP2;3	Chr4;20,411,864~20,413,318	NW_006256908.1	XM_006410834.1	XP_006410897.1	plas	plas			
EsPIP2;4	Chr6;21,418,342~21,416,629	NW_006256829.1	XM_006400761.1	XP_006400824.1	plas	plas	*Zea mays*	plas	*Zelazny et al. (2009)*
EsPIP2;5	Chr5;3,318,416~3,315,956	NW_006256858.1	XM_006403468.1	XP_006403531.1	plas	plas	*Z. mays*	plas	*Zelazny et al. (2009)*
EsPIP2;6	Chr4;21,319,556~21,322,584	NW_006256908.1	XM_006411061.1	XP_006411124.1	plas	plas	*M. nana*	plas	*Sreedharan, Shekhawat & Ganapathi (2015)*
EsPIP2;7	Chr7;27,180,960~27,182,785	NW_006256909.1	XM_006412089.1	XP_006412152.1	plas	plas	*A. thaliana*	plas	*Hachez et al. (2014)*
EsTIP1;1	Chr4;20,182,942~20,184,210	NW_006256908.1	XM_006410791.1	XP_006410854.1	vacu	cyto	*A. thaliana*	vacu	*Ma et al. (2004)*
EsTIP1;2	Chr2;16,508,526~16,506,789	NW_006256547.1	XM_006395487.1	XP_006395549.1	vacu	plas/vacu	*Eutrema salsiguneum*	vacu	*Wang et al. (2014)*
EsTIP1;3	Chr6;663,103~662,130	NW_006256756.1	XM_006396285.1	XP_006396348.1	vacu	cyto			
EsTIP2;1	Chr3;5,624,419~5,626,413	NW_006256885.1	XM_006406794.1	XP_006406857.1	vacu	chlo/vacu	*A. thaliana*	vacu	*Loque et al. (2005)*
EsTIP2;2	NA	NW_006256909.1	XM_006414179.1	XP_006414242.1	vacu	vacu	*Triticum aestivum*	vacu	*Chunhui et al. (2013)*
EsTIP2;3	Chr2;14,894,399~14,893,306	NW_006256828.1	XM_006398375.1	XP_006398438.1	vacu	vacu	*A. thaliana*	vacu	*Loque et al. (2005)*
EsTIP2;4	Chr1;27,709,976~27,708,236	NW_006256486.1	XM_006392888.1	XP_006392950.1	vacu	vacu			
EsTIP3;1	Chr5;22,490,388~22,491,488	NW_006256342.1	XM_006390520.1	XP_006390582.1	vacu	chlo/cyto/vacu	*A. thaliana*	plas/vacu	*Gattolin, Sorieul & Frigerio (2011)*
EsTIP3;2	Chr1;6,309,744~6,311,048	NW_006256612.1	XM_006416602.1	XP_006416665.1	vacu	chlo/mito/vacu	*A. thaliana*	plas/vacu	*Gattolin, Sorieul & Frigerio (2011)*
EsTIP4;1	Chr4;7,484,947~7,486,691	NW_006256895.1	XM_006408738.1	XP_006408801.1	vacu	vacu			
EsTIP5;1	Chr5;6,934,814~6,933,858	NW_006256858.1	XM_006404316.1	XP_006404379.1	vacu / plas	chlo	*A. thaliana*	mito	*Soto et al. (2010)*
EsNIP1;2	Chr7;19,890,089~19,892,520	NW_006256909.1	XM_006413978.1	XP_006414041.1	plas	plas	*A. thaliana*	plas	*Wang et al. (2017)*
EsNIP2;1	Chr4;19,043,681~19,042,522	NW_006256908.1	XM_006410521.1	XP_006410584.1	plas	vacu:	*A. thaliana*	plas/E.R	*Choi & Roberts (2007)*, *Mizutani et al. (2006)*
EsNIP3;1	Chr1;12,292,410~12,294,335	NW_006256612.1	XM_006415218.1	XP_006415281.1	plas	vacu	*O. sativa*	plas	*Hanaoka et al. (2014)*

(*continued on next page*)

Table 1 (*continued*)

Name	Chromosomal Localization	Scaffold	Coding sequence	Protein ID	Plant-mPLoc	WoLF PSORT	Plant species	Subcellular localization	Reference
EsNIP4;1	Chr7;4,484,562~4,482,986	NW_006256877.1	XM_006405767.1	XP_006405830.1	plas	plas	*A. thaliana*	plas/vacu	*DiGiorgio et al. (2016)*
EsNIP4;2	Chr7;4,513,301~4,511,485	NW_006256877.1	XM_006405768.1	XP_006405831.1	plas	plas	*A. thaliana*	plas/vacu	*DiGiorgio et al. (2016)*
EsNIP4;3	Chr7;4,481,446~4,479,745	NW_006256877.1	XM_006405766.1	XP_006405829.1	plas	plas			
EsNIP5;1	Chr6;6,005,178~6,008,910	NW_006256756.1	XM_006397006.1	XP_006397069.1	plas	plas	*A. thaliana*	plas	*Takano et al. (2006)*
EsNIP6;1	Chr5;25,383,958~25,386,014	NW_006256342.1	XM_006389768.1	XP_006389830.1	plas	plas	*A. thaliana*	plas	*Tanaka et al. (2008)*
EsNIP7;1	Chr3;1,929,290~1,927,201	NW_006256885.1	XM_006407920.1	XP_006407983.1	plas	cyto			
EsSIP1;1	Chr3;1,105,251~1,102,416	NW_006256885.1	XM_024159977.1	XP_024015745.1	plas	plas	*A. thaliana*	E.R	*Ishikawa et al. (2005)*
EsSIP1;2	Chr6;23,161,081~23,162,581	NW_006256829.1	XM_006400314.1	XP_006400377.1	vacu plas	vacu	*A. thaliana*	E.R	*Ishikawa et al. (2005)*
EsSIP2;1	Chr5;2,401,441~2,403,463	NW_006256838.1	XM_006402867.1	XP_006402930.1	plas	E.R	*A. thaliana*	E.R	*Ishikawa et al. (2005)*

Notes.

Abbreviation: plas, plasma membrane; cyto, cytosol; vacu, tonoplast membrane; chlo, chloroplast; mito, mitochondria; E.R, endoplasmic reticulum; NA, not applicable.

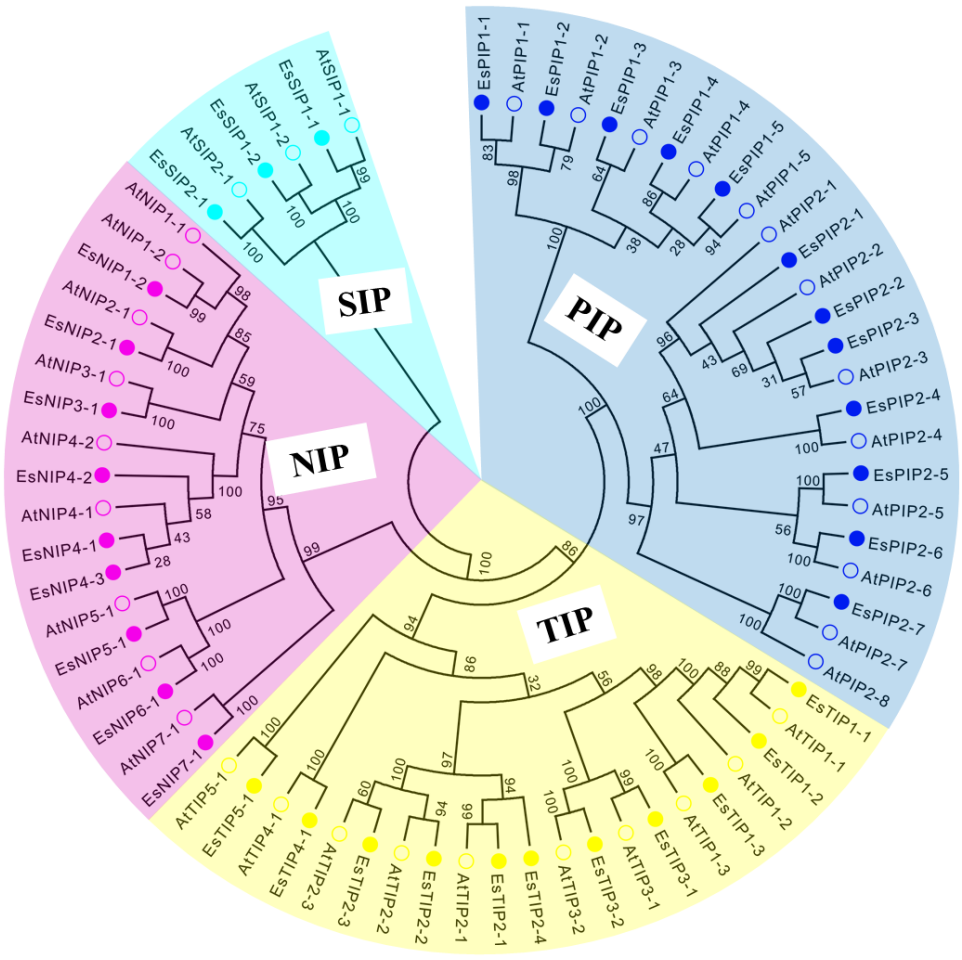

Figure 1 **Phylogenetic tree of AQP amino acid sequences from *E. salsugineum* and *A. thaliana*.** Alignments were performed using the default parameter of ClustalW and the phylogenetic tree was constructed using the Neighbor-Joining tree method with 1,000 bootstrap replicates in MEGA6.0 software. Each subfamily of AQPs was well separated in different clades and represented by different colors. The solid circle represents EsAQPs and the hollow circle represents AtAQPs.

Full-size DOI: 10.7717/peerj.7664/fig-1

Gene structure and subcellular localization analysis of EsAQPs

Gene structure analysis of the 35 *EsAQP* genes was performed on the Gene Structure Display Server of NCBI. Based on their mRNA and genomic DNA sequences, we found exon lengths were mostly conserved in each subfamily of *EsAQP* gene with same exon number, but introns varied in both length and position (Fig. 3). All members of the EsPIP subfamily contained four exons with similar length (289–328, 296, 141 and 93–126 bp, respectively) and conserved sequences in the 2nd and 3rd exon, except for *EsPIP2;4*, which had a shorter 2nd and longer 3rd exon (307, 151, 286, and 111 bp). The majority members of the EsTIP subfamily contained three exons with similar lengths, and the other members had two exons with similar lengths, except for *EsTIP1;3*, which had only one exon without intron. In the EsNIP subfamily, some members exhibited five exons with similar lengths, while others had four exons with varied lengths. All EsSIP subfamily genes displayed three

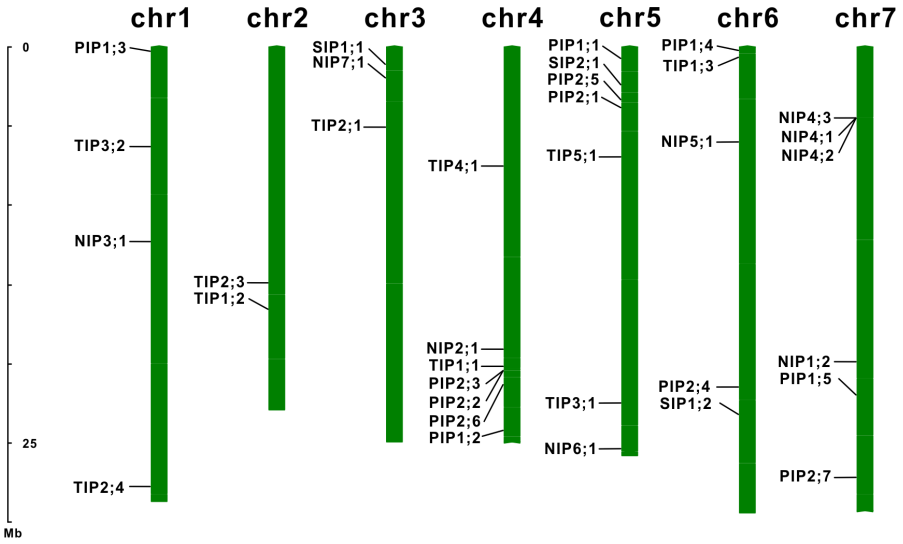

Figure 2 Chromosomal localization of the EsAQP genes. The diagram was drawn using the MapInspect software, and 34 out of 35 EsAQPs were located on seven chromosomes (except *EsTIP2;2*).
Full-size DOI: 10.7717/peerj.7664/fig-2

exons with similar lengths. This description of exon-intron structure provides additional evidence to support the classification results (*Kong et al., 2017*).

The prediction of subcellular localization showed diverse results, not always in agreement with experimentally determined localizations (reviewed in *Katsuhara et al., 2008*). In summary, the prediction of EsAQP subcellular localization in Plant-mPLoc showed that EsPIP, EsNIP and EsSIP subfamilies were localized in plasma membrane, while EsTIP subfamily members were localized in tonoplast membrane. Among them, EsPIP1;2 and EsTIP5;1 were localized in both tonoplast membrane and plasma membrane (Table 1). Moreover, WoLF PSORT predicts different location for EsAQPs and assigns values for that location (Table S4). The highest values list in Table 1 showed that EsPIPs were predicted to localize in plasma membrane, which were consistent with the Plant-mPLoc prediction and many other reports (*Cui et al., 2008*; *Hu et al., 2012*; *Xu et al., 2014*). The majority of other AQP members were predicted to localize in plasma membrane or tonoplast membrane, except for EsTIP5;1, EsNIP7;1 and EsSIP2;1, which were predicted to be associated with chloroplast, cytosol and endoplasmic reticulum, respectively. Moreover, some members showed multiple type of localization; for example, EsTIP3;1 was predicted to be associated with chloroplast/cytosol/tonoplast membrane and EsTIP3;2 with chloroplast/mitochondria/tonoplast membrane. The subcellular localization of most published AQP homologous was consistent with the predicted results in *E. salsugineum* (Table 1). These observations demonstrated that the subcellular localization of AQPs may be complex and diverse.

To verify the predictions, genes of EsPIP1;2 and EsPIP2;1 were cloned into the pBI121-GFP vector to create the 35S::EsPIP-GFP fusion proteins. The plasmid was transformed into onion epidermis by agrobacterium-mediated transformation. As shown in Fig. 4, the GFP fluorescence mainly exhibit in plasma membrane, indicated that EsPIP1;2 and

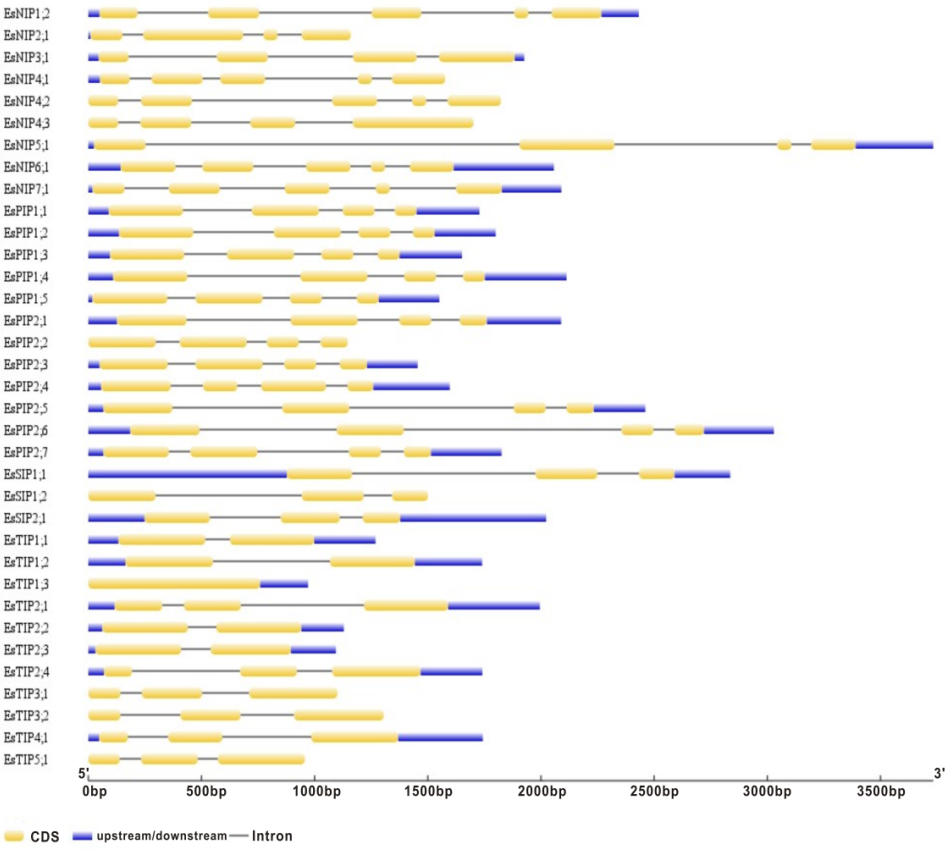

Figure 3 Gene structures of the EsAQP genes. The blue rectangle, yellow rectangle and black line represent UTR, exon and intron, respectively.

Full-size DOI: 10.7717/peerj.7664/fig-3

EsPIP2;1 proteins were consistent with the predictions. Although not conclusive, the predicted localization could serve as a useful reference for further studies on EsAQPs protein functions in plants.

Structure characteristics of EsAQPs

Sequence analysis showed that all EsAQPs contain six transmembrane domains (TMDs) comprising 237–323 amino acids, had theoretical molecular weights (MW) of 24.31–31.80 kDa and isoelectric point (pI) values of 4.73–10.49 (Table 2). The EsPIP subfamily had a similar molecular weight of approximately 30.84 kDa. Most members of the EsNIP subfamily exhibited a similar molecular weight and isoelectric point of EsPIP subfamily. The EsTIP and EsSIP subfamilies had lower MW among the EsAQPs, and the isoelectric points of these two subfamilies were acidic and alkaline, respectively (Fig. S1).

NPA motifs, ar/R selectivity filters and Froger's positions of AQP protein sequences play critical role in channel selectivity. The sequence alignment between AtAQPs and GhAQPs was carried out to analyze the conserved domains (*Quigley et al., 2001*; *Park et al., 2010*). The results in Table 2 showed that all EsPIP subfamily members had two typical NPA motifs in loop B and loop E, with a water transport ar/R filter with amino acid of F-H-T-R.

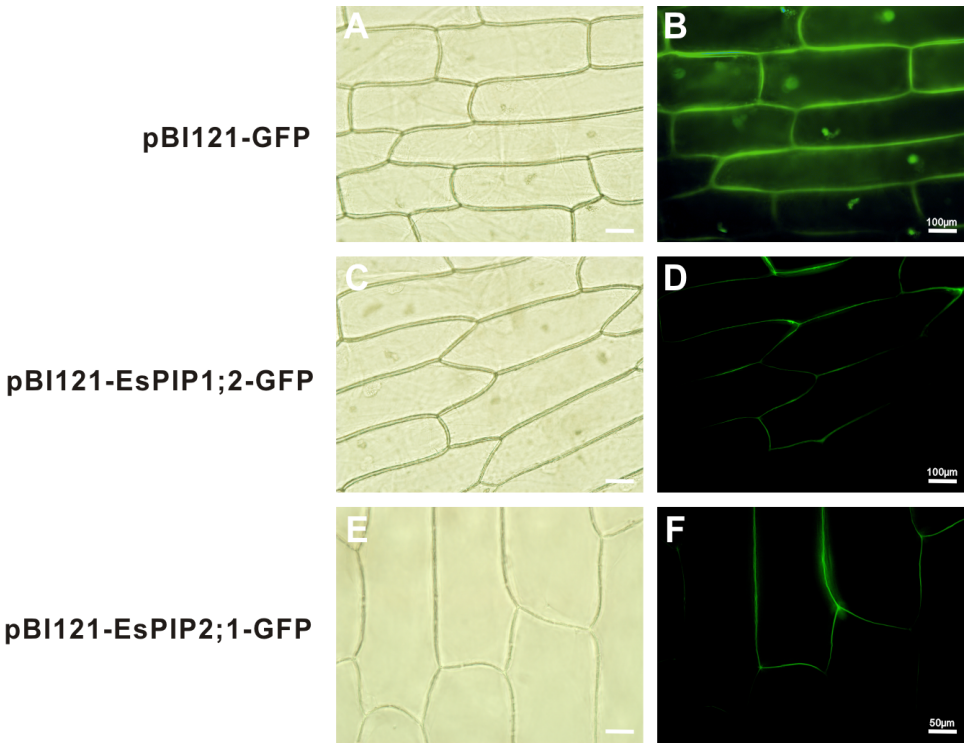

Figure 4 Subcelluar localizations of EsPIP1;2 and EsPIP2;1 proteins. Onion epidermal cells transiently transformed with empty vector (A, B), EsPIP1;2-GFP (C, D) and EsPIP2;1-GFP (E, F), respectively. The images were visualized under fluorescence microscope. A, C, E: bright-field images; B, D, F: green fluorescence images.

Full-size DOI: 10.7717/peerj.7664/fig-4

Froger's position consists of Q-S-A-F-W in most cases, except for EsPIP2;7, which had an M at the P1 position. All EsTIP subfamily had two typical NPA motifs. The ar/R was composed of H–I-A-V in EsTIP1s, H-I-G-R in EsTIP2s and H-T/M/I-A-R in other EsTIP members, while in EsTIP5;1, it was composed of N-V-G-C. Froger's position consists of T-A/S-A-Y-W, except for EsTIP5;1 and EsTIP3;2, which had a V at the P1 position and a T at the P2 position respectively. Most members of EsNIP subfamily had two typical NPA motifs, not in EsNIP2;1 (with an NPG in LE), EsNIP5;1 and EsNIP7;1 (with an NPS in LB). The ar/R filter consists of residues like W/A-V/I-A/G-R, and Froger's position consists of F-S-A-Y-L, except for EsNIP7;1, which had a Y at the P1 position, and for EsNIP5;1 and EsNIP6;1 had a T at the P2 position. The EsSIP subfamily showed a variable site in the first NPA, the alanine (A) was replaced by threonine (T), cysteine (C) or leucine (L). The ar/R filter was also inconsistent with each other: I-V-P-I in EsSIP1;1, V-F-P-I in EsSIP1;2 and S-H-G-A in EsSIP2;1. The Forger's position was composed of I-A-A-Y-W in EsSIP1s, while it was F-V-A-Y-W in EsSIP2;1.

MEME (Multiple EM for Motif Elicitation) is one of the most widely used tools for searching for novel "signals" in sets of biological sequences, include the discovery of new transcription factor binding sites and protein domains (*Bailey et al., 2006*). Conserved motifs of EsAQP proteins were predicted by MEME suite (Fig. 5). The result showed that

Table 2 Structural characteristics of the EsAQPs.

Name	AA	TM	MW(KD)	pI	NPA motif		ar/R selectivity filter				Froger's positions				
					LB	LE	H2	H5	LE1	LE2	P1	P2	P3	P4	P5
PIPs															
EsPIP1;1	286	6	30.77	9.14	NPA	NPA	F	H	T	R	Q	S	A	F	W
EsPIP1;2	286	6	30.60	9.16	NPA	NPA	F	H	T	R	Q	S	A	F	W
EsPIP1;3	286	6	30.62	9.02	NPA	NPA	F	H	T	R	Q	S	A	F	W
EsPIP1;4	286	6	30.56	9.02	NPA	NPA	F	H	T	R	Q	S	A	F	W
EsPIP1;5	287	6	30.61	9.00	NPA	NPA	F	H	T	R	Q	S	A	F	W
EsPIP2;1	287	6	30.48	6.95	NPA	NPA	F	H	T	R	Q	S	A	F	W
EsPIP2;2	284	6	30.21	6.50	NPA	NPA	F	H	T	R	Q	S	A	F	W
EsPIP2;3	285	6	30.31	6.51	NPA	NPA	F	H	T	R	Q	S	A	F	W
EsPIP2;4	285	6	30.12	7.62	NPA	NPA	F	H	T	R	Q	S	A	F	W
EsPIP2;5	286	6	30.57	8.82	NPA	NPA	F	H	T	R	Q	S	A	F	W
EsPIP2;6	290	6	31.11	7.69	NPA	NPA	F	H	T	R	Q	S	A	F	W
EsPIP2;7	281	6	29.82	9.11	NPA	NPA	F	H	T	R	M	S	A	F	W
TIPs															
EsTIP1;1	251	6	25.62	6.03	NPA	NPA	H	I	A	V	T	A	A	Y	W
EsTIP1;2	253	6	25.70	5.32	NPA	NPA	H	I	A	V	T	A	A	Y	W
EsTIP1;3	252	6	25.85	5.10	NPA	NPA	H	I	A	V	T	S	A	Y	W
EsTIP2;1	277	6	28.32	7.80	NPA	NPA	H	I	G	R	T	S	A	Y	W
EsTIP2;2	250	6	25.02	4.87	NPA	NPA	H	I	G	R	T	S	A	Y	W
EsTIP2;3	243	6	24.31	4.73	NPA	NPA	H	I	G	R	T	S	A	Y	W
EsTIP2;4	254	6	25.85	5.43	NPA	NPA	H	I	G	R	T	S	A	Y	W
EsTIP3;1	265	6	27.94	7.17	NPA	NPA	H	T	A	R	T	A	A	Y	W
EsTIP3;2	267	6	28.29	6.58	NPA	NPA	H	M	A	R	T	T	A	Y	W
EsTIP4;1	249	6	26.16	5.49	NPA	NPA	H	I	A	R	T	S	A	Y	W
EsTIP5;1	257	6	26.70	7.72	NPA	NPA	N	V	G	C	V	A	A	Y	W
NIPs															
EsNIP1;2	297	6	31.80	8.83	NPA	NPA	W	V	A	R	F	S	A	Y	L
EsNIP2;1	286	6	30.56	6.78	NPA	NPG	W	V	A	R	F	S	A	Y	L
EsNIP3;1	323	6	34.46	5.94	NPA	NPA	W	I	A	R	F	S	A	Y	L
EsNIP4;1	283	6	30.49	8.73	NPA	NPA	W	V	A	R	F	S	A	Y	L
EsNIP4;2	284	6	30.34	8.80	NPA	NPA	W	V	A	R	F	S	A	Y	L
EsNIP4;3	283	6	30.30	8.98	NPA	NPA	W	V	A	R	F	S	A	Y	L
EsNIP5;1	301	6	31.20	8.31	NPS	NPA	A	I	G	R	F	T	A	Y	L
EsNIP6;1	305	6	31.78	8.57	NPA	NPA	A	I	A	R	F	T	A	Y	L
EsNIP7;1	275	6	28.62	6.12	NPS	NPA	A	V	G	R	Y	S	A	Y	L
SIPs															
EsSIP1;1	238	6	25.41	9.89	NPT	NPA	I	V	P	I	I	A	A	Y	W
EsSIP1;2	242	6	25.96	9.83	NPC	NPA	V	F	P	I	I	A	A	Y	W
EsSIP2;1	237	6	25.85	9.64	NPL	NPA	S	H	G	A	F	V	A	Y	W

Notes.

Abbreviation: AA, amino acids length; TM, transmembrane domain; MW, molecular weight; pI, isoelectricpoint *NPA Asn-Pro-Ala motif*; ar/R, aromatic/arginine.

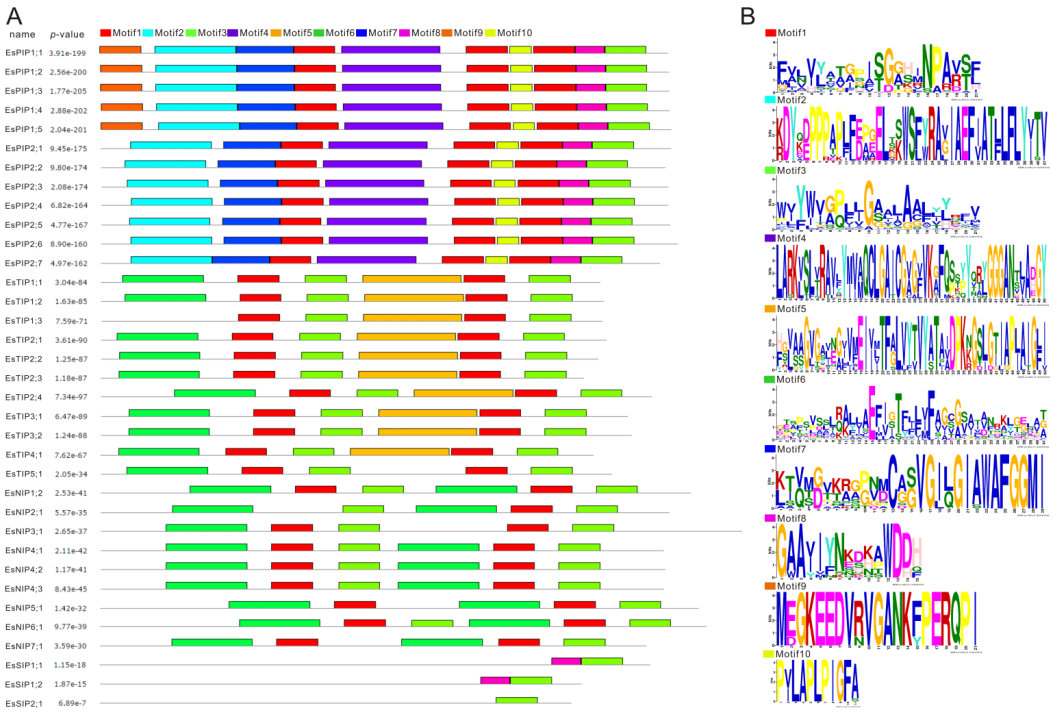

Figure 5 **Conversed motif analysis in EsAQPs.** The conversed motif prediction was identified using MEME motif search analysis, and the maximum number parameter was set to 10. Different motifs were represented by different colors. (A) Conversed motifs of 35 EsAQP proteins correspond to *p*-values. (B) Motif consensus sequences.

Full-size DOI: 10.7717/peerj.7664/fig-5

motif 1, 2, 3, 4, 7, 8, and 10 were same in all EsPIPs, and motif 2, 4, 7, and 10 were unique. In addition, motif 9 was unique in EsPIP1s and can be used to distinguish EsPIP1s from EsPIP2s. This pattern of conserved motifs in the PIP subfamily also occurs in other plants and PIP1s contain one unique motif (*Tao et al., 2014*; *Yuan et al., 2017*). In the EsTIP subfamily, almost all EsTIPs had two motif 1, two motif 3, one motif 5 and one motif 6. Except for EsTIP1;3, which had no motif 6. Motif 5 could be an identifier of EsTIPs among the AQPs of *E. salsugineum* except for EsTIP5;1. Most of members in NIP subfamily had two motif 1, two motif 3, and two motif 6, except for EsNIP2;1 (lose one motif 1), EsNIP3;1 (lose one motif 6) and EsNIP5;1 (lose one motif 3). The two motif 6 might be used to distinguish EsNIPs with other EsAQPs. All EsSIP subfamily carried motif 3. Motif 8 appeared in EsSIP1s but not in EsSIP2;1, so it might be an specific trait of this group. This is a common phenomenon in plant SIP subfamily contains less motifs (*Tao et al., 2014*; *Reddy et al., 2015*; *Yuan et al., 2017*; *Kong et al., 2017*). Based on these analysis, it was evident that there were structural differences in various EsAQP subfamilies, but conserved in their own subfamily.

Expression pattern of *EsAQPs*

The expression of *EsAQP* genes in different organs, including root, stem, leaf, flower and silique, was analyzed by RT-qPCR. The results showed that 35 *EsAQP* genes were detected

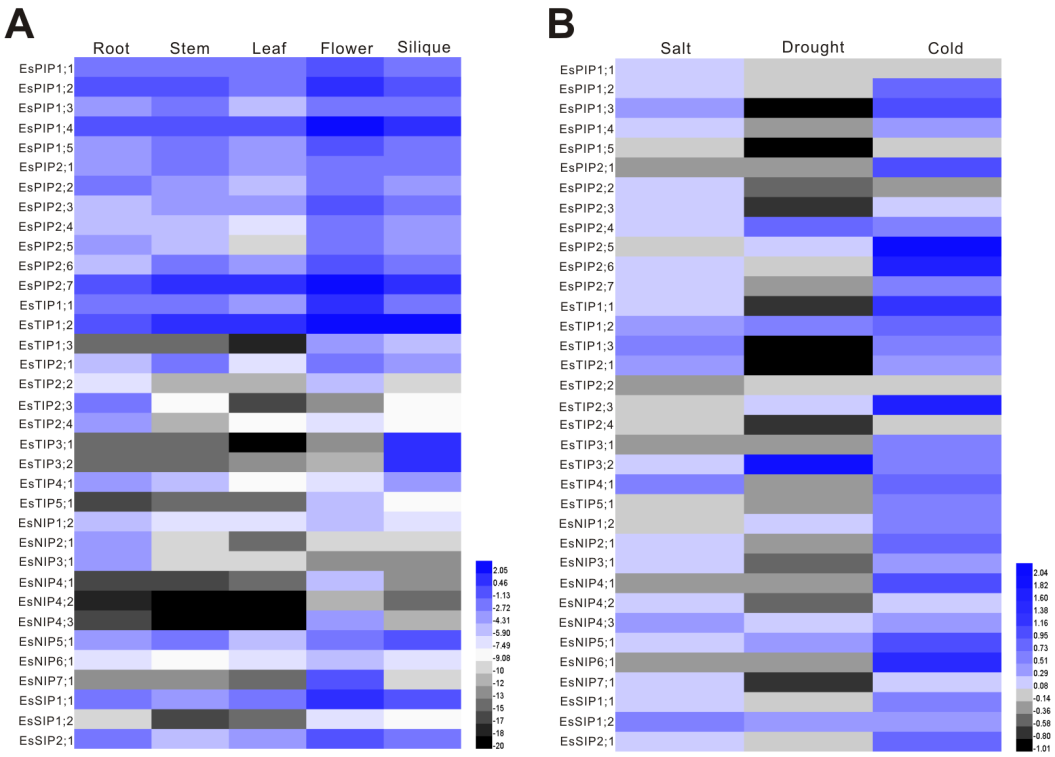

Figure 6 Expression profiles of the *EsAQP* genes. (A) *EsAQP* genes expression in response to abiotic stress. The color scale represents the $2^{-\Delta\Delta Ct}$ value normalized to untreated controls and $\log_2$ transformed counts, where green indicates downregulated expression and red indicates upregulated expression. (B) Expression of *EsAQP* genes in various organs of *E. salsugineum*. Color scales represent $2^{\Delta Ct}$ values normalized to actin and $\log_2$ transformed counts, where green indicates low expression and red indicates high expression.

Full-size DOI: 10.7717/peerj.7664/fig-6

in all the organs (Fig. 6A). Almost all *EsPIP* genes were highly expressed in all organs, except for *EsPIP2;5* in leaf. In addition, the *EsPIP* genes, *EsTIP1;1*, *EsTIP1;2*, *EsNIP1;2*, *EsNIP5;1*, *EsSIP1;1* and *EsSIP2;1* were also highly expressed in all organs. Some *EsAQP* genes, such as *EsTIP2;3*, *EsTIP2;4*, *EsNIP2;1* and *EsNIP3;1*, were specifically highly expressed in root. Two *EsTIPs* (*EsTIP2;2* and *EsTIP5;1*), three *EsNIPs* (*EsNIP4;1*, *EsNIP4;3* and *EsNIP7;1*) and *EsSIP1;2* were highly expressed only in flower. Two *EsTIPs* (*EsTIP3;1* and *EsTIP3;2*) were expressed in silique with relative high abundance. Compared analysis of each *EsAQP* gene between different organs revealed that most *EsAQP* genes showed higher expression level in flower than in other organs.

Abiotic stresses are the main limiting factors for plants during environmental conditions that induce osmotic stress and disturb water balance. AQPs play major roles in maintaining water homeostasis and responding to environmental stresses in plants. Therefore, we further investigated the expression patterns of *EsAQP* genes under salt, drought and cold stress by qRT-PCR. The results showed that most of the *EsAQP* genes were up-regulated under salt and cold stress but down-regulated under drought stress (Fig. 6B). We found that five *EsAQP* genes were up-regulated under all the types of abiotic stresses, including

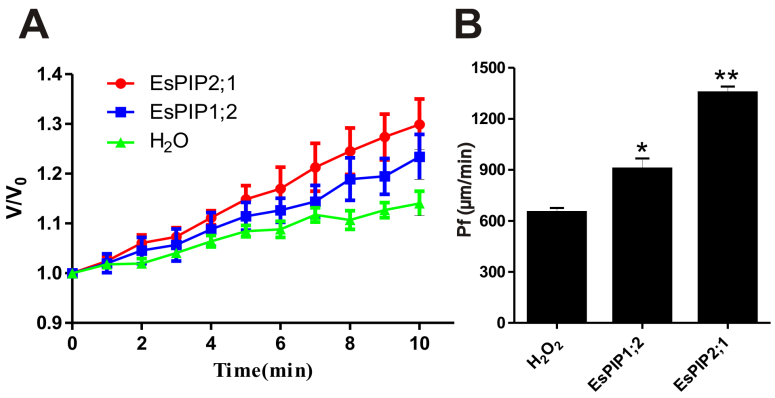

Figure 7 Water channel activity appraisals of EsPIP1;2 and EsPIP2;1. (A) The swelling rates of *Xenopus* oocytes injected with H_2O, or cRNA encoding EsPIP1;2 and EsPIP2;1, respectively. The rate of oocyte swelling upon immersion in hypo-osmotic medium is drawn as V/V_0, where V is the volume at a given time point and V_0 is the initial volume. (B) Water permeability codfficient (Pf) of oocytes injected with cRNA encoding H_2O, or EsPIP1;2, or EsPIP2;1. The Pf values were calculated from the rate of oocyte swelling. Vertical bars indicate the SE. Asterisks indicate significant differences in comparison with oocytes injected with water. Statistical analysis were performed by SPSS 16.0 using one-way ANOVA and Least Significant Difference (LSD) test to detect significant differences (*$p < 0.05$, **$p < 0.01$).

Full-size DOI: 10.7717/peerj.7664/fig-7

EsPIP2;4, *EsTIP1;2*, *EsNIP4;3*, *EsNIP5;1* and *EsSIP1;2*, while three *EsAQP* genes were down-regulated under all the types of abiotic stresses, including *EsPIP1;5*, *EsTIP2;2* and *EsTIP2;4*. In addition, *EsPIP1;1* and *EsPIP2;2* were specifically up-regulated under salt stress, and *EsPIP2;1*, *EsTIP2;1*, *EsTIP5;1*, *EsNIP4;1* and *EsNIP6;1* were up-regulated only under cold stress.

Water permeability of EsPIP1;2 and EsPIP2;1

Previously, AtPIP2;1 has been reported that is an integral membrane protein that facilitates water transport across plasma membrane while AtPIP1;2 has no function (*Li et al., 2011*; *Heckwolf et al., 2011*). To determine the water channel activity of EsPIP1;2 and EsPIP2;1, proteins were tested in the *Xenopus* oocyte system. After two days of cRNA or water injection, the change rate in oocyte volume (Fig. 7A) and the osmotic water permeability coefficient (Pf) (Fig. 7B) were calculated. Expression of EsPIP2;1 conferred a rapid osmotically driven increase in relative volume, while expression of EsPIP1;2 enabled an increase in relative volume at a slower rate than the water-injected oocytes. Compared with water-injected control, the oocytes expressing EsPIP1;2 and EsPIP2;1 showed 1.39-fold and 2.08-fold increase in Pf, suggesting that both EsPIP1;2 and EsPIP2;1 are functional AQP with water channel activity. Meanwhile, our result is consistent with the known information that PIP2s have high efficiency water transfer activity but PIP1s have little or no increase in the Pf (*Chaumont & Tyerman, 2014*).

DISCUSSION

Gene duplication is a ubiquitous event that plays an important role in biological evolution, which may also contribute to stress tolerance via gene dosage increasing, avoiding some

deleterious mutations and creating the opportunity for new function emergence (*Innan & Kondrashov, 2010*). AQPs are abundant, diverse and widely distributed in plants and involved in regulation of plant growth and development. From algae (two in *Thalassiosira pseudonana* and five in *Phaeodactylum tricornutum*) (*Armbrust et al., 2004*; *Bowler et al., 2008*) to fern (19 in *Selaginella moellendorffii*) (*Danielson & Johanson, 2008*) and moss (23 in *Physcomitrella patens*) (*Anderberg, Kjellbom & Johanson, 2012*) to higher plants (35 AQPs in *Arabidopsis*, 33 in *Oryza sativa*, 72 in *Glycine max*) (*Johanson et al., 2001*; *Sakurai et al., 2005*; *Zhang et al., 2013*), the number of AQPs has largely increased with evolution. Here, we provide a genome-wide information of AQP family of *E. salsugineum*.

In previous studies, it was shown that more than 95% gene families are shared in *T. salsuginea* (the former name of *E. salsugineum*, *Koch & German, 2013*) with *A. thaliana* (*Wu et al., 2012*) or more than 80% *E. salsugineum* genes had high homology orthologs in *A. thaliana* (*Yang et al., 2013*). The number of AQPs identified in *E. salsugineum* is the same as that in *A. thaliana*, and their protein sequences have very high similarities. No homologies of AtAQPs, PIP2;8 and NIP1;1 were not identified in *E. salsugineum*, while another two AQPs, TIP2;4 and NIP4;3 were found instead, which were not existed in *Arabidopsis*. These differences may not be directly illustrated the superiority of *E. salsugineum* in stress resistance, the functions of EsAQPs in resistance need to be further studied.

Structural analysis and functional inference of EsAQPs

Exon-intron structural divergence commonly happened in duplicate gene evolution and even in sibling paralogs; these changes occurred through the mechanisms of gain/loss, exonization/pseudoexonization and insertion/deletion (*Xu et al., 2012*). In common bean (*Phaseolus vulgaris* L.), each aquaporin subfamily are completely conserved in number, order and length of exons but varies in introns (*Ariani & Gepts, 2015*). The MEME motifs of the AQPs were conserved in all subfamilies, while a few were deleted, unique or family-specific, and a previous report also found this pattern in ZmPIPs (*Bari et al., 2018*). In our study, the exon-intron structure of *EsAQP* genes and the conserved MEME motifs of EsAQP protein sequences showed some common patterns (Figs. 3 and 5). These results indicated that the gene structure and the conserved motifs of EsAQPs shown subfamily-specific, these traits may provide new evidence to support the classification.

High conservation of signature sequences or residues was shown in plant PIP proteins. In our study (Table 2), EsPIPs showed a typical NPA motif, a highly conserved ar/R selectivity filter and Froger's position of F-H-T-R and Q/M-S-A-F-W, these characteristics are correlated with water transport activity (*Quigley et al., 2001*). In addition to water transport, plant PIPs also could transfer carbon dioxide, hydrogen peroxide, boric acid, and urea (*Gaspar et al., 2003*; *Bienert et al., 2014*; *Heckwolf et al., 2011*). According to the SDP analysis proposed by *Hove & Bhave (2011)*, all EsPIPs had H_2O_2-type and urea-type SDPs (Table 3, Fig. S2). In addition, all EsPIP1s and EsPIP2;5 had boric acid-type SDPs, and all EsPIP1s had CO_2-type SDPs, including two novel types of SDP showed in EsPIP1;3 and EsPIP1;4 which have an M in place of I in SDP2, it also have been found in RcPIPs, JcPIPs and BvPIPs (*Zou et al., 2015*; *Zou et al., 2016*; *Kong et al., 2017*). In addition, EsPIP2;4 owned another novel CO_2-type SDPs (V-I-C-A-V-E-W-D-W), with E replaced by D in

Table 3 Identified typical SDPs in EsAQPs. The red font represent novel site.

Aquaporin	Specificity-determining positions								
	SDP1	**SDP2**	**SDP3**	**SDP4**	**SDP5**	**SDP6**	**SDP7**	**SDP8**	**SDP9**
Ammonia Transporters	**F/T**	**K/L/N/V**	**F/T**	**V/L/T**	**A**	**D/S**	**A/H/L**	**E/P/S**	**A/R/T**
EsTIP2;1	T	L	T	V	A	S	H	P	A
EsTIP3;1	T	L	G	T	A	S	H	P	A
EsNIP1;2	F	K	F	T	G	D	L	E	T
EsNIP4;1	F	T	F	T	A	D	L	E	T
EsNIP4;3	F	T	F	T	A	D	L	E	T
Boric Acid transporter	**T/V**	**I/V**	**H/I**	**P**	**E**	**I/L**	**I/L/T**	**A/T**	**A/G/P/K**
EsPIP1;1	T	I	H	P	E	L	L	T	P
EsPIP1;2	T	I	H	P	E	L	L	T	P
EsPIP1;3	T	I	H	P	E	L	L	T	P
EsPIP1;4	T	I	H	P	E	L	L	T	P
EsPIP1;5	T	I	H	P	E	L	L	T	P
EsPIP2;5	T	I	H	P	E	L	L	T	P
EsNIP5;1	T	I	H	P	E	L	L	A	P
EsNIP6;1	T	I	H	P	E	L	L	A	P
EsNIP7;1	V	I	H	P	E	L	L	T	P
CO_2 transporter	**I/L/V**	**I**	**C**	**A**	**I/V**	**D**	**W**	**D**	**W**
EsPIP1;1	L	I	C	A	I	D	W	D	W
EsPIP1;2	V	I	C	A	I	D	W	D	W
EsPIP1;3	V	M	C	A	I	D	W	D	W
EsPIP1;4	V	M	C	A	I	D	W	D	W
EsPIP1;5	V	I	C	A	I	D	W	D	W
EsPIP2;4	V	I	C	A	V	E	W	D	W
H_2O_2 transporters	**A/S**	**A/G**	**L/V**	**A/F/L/V/T**	**I/L/V**	**H/I/L/Q**	**F/Y**	**A/V**	**P**
EsPIP1;1	A	G	V	F	I	H	F	V	P
EsPIP1;2	A	G	V	F	I	H	F	V	P
EsPIP1;3	A	G	V	F	I	H	F	V	P
EsPIP1;4	A	G	V	F	I	H	F	V	P
EsPIP1;5	A	G	V	F	I	H	F	V	P
EsPIP2;1	A	G	V	F	I	H	F	V	P
EsPIP2;2	A	G	V	F	I	H	F	V	P
EsPIP2;3	A	G	V	F	I	H	F	V	P
EsPIP2;4	A	G	V	F	I	Q	F	V	P
EsPIP2;5	A	G	V	F	I	H	F	V	P
EsPIP2;6	A	G	V	F	I	Q	F	V	P
EsPIP2;7	A	G	V	F	I	H	F	V	P
EsTIP1;1	S	A	L	A	I	H	Y	A	P
EsTIP1;2	S	A	L	A	I	H	Y	A	P
EsTIP1;3	A	A	L	S	I	H	Y	V	P
EsTIP2;1	S	A	L	V	I	H	Y	V	P

(*continued on next page*)

Table 3 (*continued*)

Aquaporin	Specificity-determining positions								
	SDP1	SDP2	SDP3	SDP4	SDP5	SDP6	SDP7	SDP8	SDP9
EsTIP2;2	S	A	L	V	I	I	Y	V	P
EsTIP2;3	S	A	L	V	I	I	Y	V	P
EsTIP3;2	A	A	L	A	I	H	Y	V	P
EsTIP4;1	S	A	L	L	T	H	Y	V	P
EsNIP1;2	S	A	L	L	V	I	Y	V	P
EsNIP3;1	S	A	L	V	I	L	Y	V	P
EsNIP5;1	S	A	L	V	V	L	Y	V	P
Silicic acid transporters	**C/S**	**F/Y**	**A/E/L**	**H/R/Y**	**G**	**K/N/T**	**R**	**E/S/T**	**A/K/P/T**
Not found									
Urea Transporters	**H**	**P**	**F/I/L/T**	**A/C/F/L**	**L/M**	**A/G/P**	**G/S**	**G/S**	**N**
EsPIP1;1	H	P	F	F	L	P	G	G	N
EsPIP1;2	H	P	F	F	L	P	G	G	N
EsPIP1;3	H	P	F	F	L	P	G	G	N
EsPIP1;4	H	P	F	F	L	P	G	G	N
EsPIP1;5	H	P	F	F	L	P	G	G	N
EsPIP2;1	H	P	F	F	L	P	G	G	N
EsPIP2;2	H	P	F	F	L	P	G	G	N
EsPIP2;3	H	P	F	F	L	P	G	G	N
EsPIP2;4	H	P	F	F	L	P	G	G	N
EsPIP2;5	H	P	F	F	L	P	G	G	N
EsPIP2;6	H	P	F	F	L	P	G	G	N
EsPIP2;7	H	P	F	F	L	P	G	G	N
EsTIP1;1	H	P	F	F	L	A	G	S	N
EsTIP1;2	H	P	F	F	L	A	G	S	N
EsTIP1;3	H	P	F	F	L	A	G	S	N
EsTIP2;1	H	P	F	A	L	P	G	S	N
EsTIP2;2	H	P	L	A	L	P	G	S	N
EsTIP2;3	H	P	L	A	L	P	G	S	N
EsTIP2;4	H	P	F	V	L	P	G	S	N
EsTIP3;1	H	P	F	L	L	P	G	S	N
EsTIP3;2	H	P	L	L	L	P	G	S	N
EsTIP4;1	H	P	I	L	L	A	G	S	N
EsTIP5;1	H	P	F	A	L	P	G	S	N
EsNIP1;2	H	P	I	A	L	P	G	S	N
EsNIP2;1	H	P	I	A	L	E	G	S	N
EsNIP3;1	H	P	I	A	L	P	G	S	N
EsNIP4;1	H	P	V	A	L	P	G	S	N
EsNIP4;2	H	P	F	A	L	P	G	S	N
EsNIP4;3	H	P	I	A	L	P	G	S	N
EsNIP5;1	H	P	I	A	L	P	G	S	N
EsNIP6;1	H	P	I	A	L	P	S	S	N
EsNIP7;1	H	P	I	A	V	P	G	S	N

SDP6. These results showed the conservation of plant PIPs in the transport of urea and hydrogen peroxide (*Gaspar et al., 2003*; *Bienert et al., 2014*), and PIP1s not PIP2s are main CO_2 and boric acid channels (*Heckwolf et al., 2011*).

Compared to PIPs, TIPs are more diverse which have a variety of selectivity filters. Two typical NPA motifs were found in all the EsTIPs, and the ar/R filters and Froger's position were conserved in the EsTIP1s and EsTIP2s classes, but different with other classes. All the EsTIPs showed urea-type SDPs, and most of them had H_2O_2-type SDPs (except for EsTIP3;1 and EsTIP5;1). EsTIP2;1 had an NH_3-type SDPs, as confirmed in *Arabidopsis* TIP2;1 (*Loque et al., 2005*). EsTIP3;1 possessed a novel NH_3-type SDPs (T-L-G-T-A-S-H-P-A) with F/T replaced by G in SDP3. The NIP subfamily has low intrinsic water permeability and the ability to transport solutes like glycerol and ammonia (*Choi & Roberts, 2007*). Most EsNIPs held two typical NPA motifs, but some varied at the third residue in the first or second NPA motif. All EsNIPs had urea-type SDPs, EsNIP1;2, EsNIP3;1 and EsNIP5;1 had H_2O_2-type SDPs. EsNIP5;1, EsNIP6;1 and EsNIP7;1 had boric acid-type SDPs, which have been found in *Arabidopsis* (*Takano et al., 2006*). EsNIP1;2 possessed a novel NH_3-type SDPs with a substitution of G for A at SDP4. In addition, EsNIP4;1 and EsNIP4;3, which both had the substitution of T for K/L/N/V at SDP2. EsSIPs varied in the third residue of the first NPA motif, with diverse ar/R filters and Froger's positions. However, the residues were consistent with the corresponding SIP in *Arabidopsis*. AtSIP1;1 and AtSIP1;2 could transport water in the ER. AtSIP2;1 might act as an ER channel for other small molecules or ions (*Ishikawa et al., 2005*), and their similarity in these motifs suggests that these EsSIPs may have similar function. These results indicate that the diversity of AQPs in *E. salsugineum* may have crucial role in response to environmental stress.

Distinct expression profiles of *EsAQP* genes in various organs

Previous studies have shown that many AQPs show similar expression patterns, suggesting that they may act synergistic in some organs. For instance, PIPs and TIPs are abundant in all organs in many plant species (*Quigley et al., 2001*; *Venkatesh, Yu & Park, 2013*; *Reuscher et al., 2013*; *Zou et al., 2015*; *Yuan et al., 2017*). The qRT-PCR results showed that the transcripts of *EsAQP* genes could be detected in all organs, but their expression levels were diverse (Fig. 6A). Among them, the most abundant transcripts were *EsPIPs* and a few *EsTIPs* (*EsTIP1;1* and *EsTIP1;2*), which were consistent with previous studies, especially with *Arabidopsis AQP* genes (*Jang et al., 2004*). The high expression of these *AQP* genes may be related to their effective water channel function that mediates water uptake in plant (*Jang et al., 2004*; *Gomes et al., 2009*). Moreover, *EsTIP3;1* and *EsTIP3;2* were highly expressed in silique specifically. It has been reported that seed-specific TIP3;1 and TIP3;2 play a role in maintaining seed longevity, and as target genes of ABI3 transcription factor which known to be involved in seed desiccation tolerance and seed longevity (*Mao & Sun, 2015*). It suggested that TIP3s may be involve in cellular osmoregulation and maturation of the vacuolar apparatus to support optimal water uptake and growth of the embryo during seed development and germination (*Shivaraj et al., 2017*). In general, the transcript level of NIP subfamily is lower than others. However, the *EsNIP5;1* was high abundant in all organs, and some of them showed organ specific. For example, *EsNIP2;1* and

EsNIP3;1 were predominant expression in root, *EsNIP4;1*, *EsNIP4;1* and *EsNIP7;1* were predominantly expressed in flower. These may rely on their transport function of diverse substrates (*Mitani-Ueno et al., 2011*). Strikingly, the *SIP1;1* and *SIP2;1* exhibited higher expression than many *TIPs* and *NIPs* in both *E. salsugineum* (this study) and *Arabidopsis* (*Alexandersson et al., 2005*). Compared with different organs, many *AQP* genes are mainly expressed in roots and flowers, whereas no *AQP* isoform is leaf specific in *Arabidopsis* (*Alexandersson et al., 2005*). These results were also observed in our investigation. Above all, the parallel expression patterns of *AQP* genes in different organs between *E. salsugineum* and *Arabidopsis* may further indicated their similarity.

Stress responsive *AQP* genes in *E. salsugineum*

Environmental stress factors such as salt, drought and low temperature can quickly reduce water transport rates (*Javot & Maurel, 2002*), thus the maintenance of osmotic potential is a major challenge for plants. Since AQPs are known to be involved in the maintenance of water balance in the plant, we investigated the expression of *EsAQP* genes at aerial parts of seedlings under various abiotic stresses including salt, drought and cold. In *Arabidopsis*, most *AQP* genes are down-regulated upon drought stress in leaves, with the exception of *AtPIP1;4* and *AtPIP2;5*, which are up-regulated (*Alexandersson et al., 2005*). Besides, the expression analysis of *AtPIPs* at aerial parts show that only the PIP2;5 was up-regulated by cold treatment, and most of the *AtPIP* genes were down-regulated by cold stress whereas less-severely modulated by high salinity (*Jang et al., 2004*). In our data (Fig. 6B), major *AQP* genes of *E. salsugineum* were down-regulated expression to drought treatment, however, nine genes (*EsPIP2;4*, *EsPIP2;5*, *EsTIP1;2*, *EsTIP2;3*, *EsTIP3;2*, *EsNIP1;2*, *EsNIP4;3*, *EsNIP5;1* and *EsSIP1;2*) were up-regulated. Among these, the level of *EsTIP3;2* was most significantly increased after drought treatment, which has low abundance in leaf (Fig. 6A). It is suggested that *EsTIP3;2* may play a unique role under drought stress. While most of *AQP* genes were up-regulated under salt stress, it is consistent with those in barley and bamboo (*Hove et al., 2015*; *Sun et al., 2016*). Contrary to *Arabidopsis*, most of *AQP* genes in *E. salsugineum* were up-regulated under cold stress. This type of expression pattern has been reported in *Sorghum bicolor* (*Reddy et al., 2015*), to improve water transport efficiency and enhance cold tolerance (*Li et al., 2008*). Moreover, *EsPIP1;5* was down-regulated under abiotic stresses but highly abundant in all organs, the *EsTIP1;2* and *EsNIP5;1* were highly abundant in all organs and up-regulated under various stresses. These *AQP* genes were induced by external stimuli, and implied to play role in maintaining water homeostasis during environmental stress (*Jang et al., 2004*).

CONCLUSIONS

In our study, a genome-wide information of *E. salsugineum AQP* gene family was provided. 35 *EsAQP* s, located in seven chromosomes, were identified and divided into four subfamilies based on phylogenetic analysis, which was also supported by the subfamily-specific gene structure and MEME motifs analysis. Furthermore, functional properties were investigated through the analysis of ar/R filters, Froger's positions and SDPs, which have potential outputs for the widely function of EsAQPs. Moreover, the expression analysis was

performed by qRT-PCR, showing *AQP* genes were widely involved in *E. salsugineum* organs development and abiotic stress response, and may have the potentially important roles in *E. salsugineum*. Our work not only provided a full-scale bioinformation of *E. salsugineum AQP* genes, but also offered a positive assessment for the underlying candidate EsAQPs in abiotic stress response.

ACKNOWLEDGEMENTS

The authors appreciate those contributors who make the *Eutrema salsugineum* genome data accessible in public databases.

ADDITIONAL INFORMATION AND DECLARATIONS

Funding

This work was supported by the National Natural Science Foundation of China (No. 31570396) and the Fundamental Research Funds for the Central Universities (2572016DA05). The funders had no role in study design, data collection and analysis, decision to publish, or preparation of the manuscript.

Grant Disclosures

The following grant information was disclosed by the authors:
National Natural Science Foundation of China: 31570396.
Fundamental Research Funds for the Central Universities: 2572016DA05.

Competing Interests

The authors declare there are no competing interests.

Author Contributions

- Weiguo Qian conceived and designed the experiments, performed the experiments, analyzed the data, contributed reagents/materials/analysis tools, prepared figures and/or tables, authored or reviewed drafts of the paper, approved the final draft.
- Xiaomin Yang, Jiawen Li and Rui Luo performed the experiments.
- Xiufeng Yan conceived and designed the experiments, contributed reagents/materials/-analysis tools, approved the final draft.
- Qiuying Pang conceived and designed the experiments, contributed reagents/materials/analysis tools, authored or reviewed drafts of the paper, approved the final draft.

Data Availability

The following information was supplied regarding data availability:

The primers used in qRT-PCR are available in Table S1. The specificity determining positions (SDPs) analysis of *E.salsugineum* AQPs from alignments with putative amino acid sequences of AQPs transporting non-aqua substrates are available in Fig. S2.

Supplemental Information

Supplemental information for this article can be found online at http://dx.doi.org/10.7717/peerj.7664#supplemental-information.

REFERENCES

Alexandersson E, Fraysse L, Sjövall-Larsen S, Gustavsson S, Fellert M, Karlsson M, Johanson U, Kjellbom P. 2005. Whole gene family expression and drought stress regulation of aquaporins. *Plant Molecular Biology* **59**:469–484 DOI 10.1007/s11103-005-0352-1.

Anderberg HI, Kjellbom P, Johanson U. 2012. Annotation of *Selaginella moellendorffii* major intrinsic proteins and the evolution of the protein family in terrestrial plants. *Frontiers in Plant Science* **3**:Article 33 DOI 10.3389/fpls.2012.00033.

Ariani A, Gepts P. 2015. Genome-wide identification and characterization of aquaporin gene family in common bean (*Phaseolus vulgaris*, L.). *Molecular Genetics & Genomics* **290**:1771–1785 DOI 10.1007/s00438-015-1038-2.

Armbrust EV, Berges JA, Bowler C, Green BR, Martinez D, Putnam NH, Zhou S, Allen AE, Apt KE, Bechner M, Brzezinski MA, Chaal BK, Chiovitti A, Davis AK, Demarest MS, Detter JC, Glavina T, Goodstein D, Hadi MZ, Hellsten U, Hildebrand M, Jenkins BD, Jurka J, Kapitonov VV, Kröger N, Lau WW, Lane TW, Larimer FW, Lippmeier JC, Lucas S, Medina M, Montsant A, Obornik M, Parker MS, Palenik B, Pazour GJ, Richardson PM, Rynearson TA, Saito MA, Schwartz DC, Thamatrakoln K, Valentin K, Vardi A, Wilkerson FP, Rokhsar DS. 2004. The Genome of the diatom *Thalassiosira pseudonana*: ecology, evolution, and metabolism. *Science* **306**:79–86 DOI 10.1126/science.1101156.

Bailey TL, Williams N, Misleh C, Li WW. 2006. Meme: discovering and analyzing dna and protein sequence motifs. *Nucleic Acids Research* **34**:W369–W373 DOI 10.1093/nar/gkl198.

Bansal A, Sankararamakrishnan R. 2007. Homology modeling of major intrinsic proteins in rice, maize and *Arabidopsis*: comparative analysis of transmembrane helix association and aromatic/arginine selectivity filters. *BMC Structural Biology* **7**:27–27 DOI 10.1186/1472-6807-7-27.

Bari A, Farooq M, Hussain A, Muhammad TUQ, Abbas MW, Mustafa G, Karim A, Ahmed I, Hussain T. 2018. Genome-wide bioinformatics analysis of aquaporin gene family in maize (*Zea mays* L.). *Journal of Phylogenetics & Evolutionary Biology* **6**:Article 197 DOI 10.4172/2329-9002.1000197.

Biela A, Grote K, Otto B, Hoth S, Hedrich R, Kaldenhoff R. 1999. The *Nicotiana tabacum* plasma membrane aquaporin NtAQP1 is mercury-insensitive and permeable for glycerol. *Plant Journal* **18**:565–570 DOI 10.1046/j.1365-313X.1999.00474.x.

Bienert GP, Heinen RB, Berny MC, Chaumont F. 2014. Maize plasma membrane aquaporin ZmPIP2;5, but not ZmPIP1;2, facilitates transmembrane diffusion of hydrogen peroxide. *Biochimica et Biophysica Acta* **1838**:216–222 DOI 10.1016/j.bbamem.2013.08.011.

Bowler C, Allen AE, Badger JH, Grimwood J, Jabbari K, Kuo A, Maheswari U, Martens C, Maumus F, Otillar RP, Rayko E, Salamov A, Vandepoele K, Beszteri B, Gruber A, Heijde M, Katinka M, Mock T, Valentin K, Verret F, Berges JA, Brownlee C, Cadoret JP, Chiovitti A, Choi CJ, Coesel S, De Martino A, Detter JC, Durkin

C, Falciatore A, Fournet J, Haruta M, Huysman MJ, Jenkins BD, Jiroutova K, Jorgensen RE, Joubert Y, Kaplan A, Kröger N, Kroth PG, La Roche J, Lindquist E, Lommer M, Martin-Jézéquel V, Lopez PJ, Lucas S, Mangogna M, McGinnis K, Medlin LK, Montsant A, Oudot-Le Secq MP, Napoli C, Obornik M, Parker MS, Petit JL, Porcel BM, Poulsen N, Robison M, Rychlewski L, Rynearson TA, Schmutz J, Shapiro H, Siaut M, Stanley M, Sussman MR, Taylor AR, Vardi A, von Dassow P, Vyverman W, Willis A, Wyrwicz LS, Rokhsar DS, Weissenbach J, Armbrust EV, Green BR, Van de Peer Y, Grigoriev IV. 2008. The *Phaeodactylum* genome reveals the evolutionary history of diatom genomes. *Nature* **456**:239–244 DOI 10.1038/nature07410.

Chaumont F, Tyerman SD. 2014. Aquaporins: highly regulated channels controlling plant water relations. *Plant Physiology* **164**:1600–1618 DOI 10.1104/pp.113.233791.

Choi WG, Roberts DM. 2007. *Arabidopsis* NIP2;1, a major intrinsic protein transporter of lactic acid induced by anoxic stress. *Journal of Biological Chemistry* **282**:24209–24218 DOI 10.1074/jbc.M700982200.

Chunhui X, Meng W, Li Z, Taiyong Q, Guangmin X, Jauhar A. 2013. Heterologous expression of the wheat aquaporin gene TaTIP2;2 compromises the abiotic stress tolerance of *Arabidopsis thaliana*. *PLOS ONE* **8**:e79618 DOI 10.1371/journal.pone.0079618.

Cui XH, Hao FS, Chen H, Chen J, Wang XC. 2008. Expression of the *Vicia faba* Vf-PIP1gene in *Arabidopsis thaliana* plants improves their drought resistance. *Journal of Plant Research* **121**:207–214 DOI 10.1007/s10265-007-0130-z.

Danielson JÅ, Johanson U. 2008. Unexpected complexity of the aquaporin gene family in the moss *Physcomitrella patens*. *BMC Plant Biology* **8**:45 DOI 10.1186/1471-2229-8-45.

Deokar AA, Tar'an B. 2016. Genome-wide analysis of the aquaporin gene family in Chickpea (*Cicer arietinum* L.). *Frontiers in Plant Science* **7**:Article 1802 DOI 10.3389/fpls.2016.01802.

Dev TB, Herbert JK. 2018. From aquaporin to ecosystem: plants in the water cycle. *Journal of Plant Physiology* **227**:1–2 DOI 10.1016/j.jplph.2018.06.008.

DiGiorgio JA, Bienert GP, Ayub ND, Yaneff A, Barberini ML, Mecchia MA, Amodeo G, Soto GC, Muschietti JP. 2016. Pollen-specific aquaporins NIP4;1 and NIP4;2 are required for pollen development and pollination in Arabidopsis thaliana. *The Plant Cell* **28**:1053–1077 DOI 10.1105/tpc.15.00776.

Dynowski M, Schaaf G, Loque D, Moran O, Ludewig U. 2008. Plant plasma membrane water channels conduct the signaling molecule H_2O_2. *Biochemical Journal* **414**:53–61 DOI 10.1042/BJ20080287.

Feng ZJ, Xu SC, Liu N, Zhang GW, Hu QZ, Xu ZS, Gong YM. 2017. Identification of the AQP members involved in abiotic stress responses from *Arabidopsis*. *Gene* **646**:64–73 DOI 10.1016/j.gene.2017.12.048.

Fortin MG, Morrison NA, Verma DPS. 1987. Nodulin-26, a peribacteroid membrane nodulin is expressed independently of the development of the peribacteroid compartment. *Nucleic Acids Research* **15**:813–824 DOI 10.1093/nar/15.2.813.

Froger A, Tallur B, Thomas D, Delamarche C. 1998. Prediction of functional residues in water channels and related proteins. *Protein Science* **7**:1458–1468 DOI 10.1002/pro.5560070623.

Gaspar M, Bousser A, Sissoëff I, Roche O, Hoarau J, Mahé A. 2003. Cloning and characterization of ZmPIP1-5b, an aquaporin transporting water and urea. *Plant Science* **165**:21–31 DOI 10.1016/j.jinsphys.2013.08.013.

Gattolin S, Sorieul M, Frigerio L. 2011. Mapping of tonoplast intrinsic proteins in maturing and germinating Arabidopsis seeds reveals dual localization of embryonic TIPs to the tonoplast and plasma membrane. *Molecular Plant* **4**:180–189 DOI 10.1093/mp/ssq051.

Gerbeau P, Guclu J, Ripoche P, Maurel C. 1999. Aquaporin Nt-TIPa can account for the high permeability of tobacco cell vacuolar membrane to small neutral solutes. *Plant Journal* **18**:577–587 DOI 10.1046/j.1365-313x.1999.00481.x.

Gomes D, Agasse A, Thiébaud P, Delrot S, Gerós H, Chaumont F. 2009. Aquaporins are multifunctional water and solute transporters highly divergent in living organisms. *Biochimica et Biophysica Acta* **1788**:1213–1228 DOI 10.1016/j.bbamem.2009.03.009.

Gustavsson S, Lebrun AS, Kristina N, François C, Johanson U. 2005. A novel plant major intrinsic protein in *Physcomitrella patens* most similar to bacterial glycerol channels. *Plant Physiology* **139**:287–295 DOI 10.1104/pp.105.063198.

Hachez C, Laloux T, Reinhardt H, Cavez D, Degand H, Grefen C, Rycke RD, Inzé D, Blatt MR, Russinova E, Chaumont F. 2014. *Arabidopsis* SNAREs SYP61 and SYP121 coordinate the trafficking of plasma membrane aquaporin PIP2;7 to modulate the cell membrane water permeability. *The Plant Cell* **26**:3132–3147 DOI 10.1105/tpc.114.127159.

Hanaoka H, Uraguchi S, Takano J, Tanaka M, Fujiwara T. 2014. OsNIP3;1, a rice boric acid channel, regulates boron distribution and is essential for growth under boron-deficient conditions. *The Plant Journal* **78**:890–902 DOI 10.1111/tpj.12511.

Heckwolf M, Pater D, Hanson DT, Kaldenhoff R. 2011. The *Arabidopsis thaliana* aquaporin AtPIP1;2 is a physiologically relevant CO_2 transport facilitator. *Plant Journal* **67**:795–804 DOI 10.1111/j.1365-313X.2011.04634.x.

Hove RM, Bhave M. 2011. Plant aquaporins with non-aqua functions: deciphering the signature sequences. *Plant Molecular Biology* **75**:413–430 DOI 10.1007/s11103-011-9737-5.

Hove RM, Mark Z, Mrinal B, Ricardo A. 2015. Identification and expression analysis of the barley (*Hordeum vulgare* L.) aquaporin gene family. *PLOS ONE* **10**:e0128025 DOI 10.1371/journal.pone.0128025.

Hu W, Yuan Q, Wang Y, Cai R, Deng X, Wang J, Zhou S, Chen M, Chen L, Huang C, Ma Z, Yang G, He G. 2012. Overexpression of a wheat aquaporin gene, TaAQP8, enhances salt stress tolerance in transgenic Tobacco. *Plant and Cell Physiology* **53**:2127–2141 DOI 10.1093/pcp/pcs154.

Inan G, Zhang Q, Li P, Wang Z, Cao Z, Zhang H, Zhang C, Quist TM, Goodwin SM, Zhu J, Shi H, Damsz B, Charbaji T, Gong Q, Ma S, Fredricksen M, Galbraith DW, Jenks MA, Rhodes D, Hasegawa PM, Bohnert HJ, Joly RJ, Bressan RA, Zhu

JK. 2004. Salt Cress. A halophyte and cryophyte *Arabidopsis* relative model system and its applicability to molecular genetic analyses of growth and development of extremophiles. *Plant Physiology* **135**:1718–1737 DOI 10.1104/pp.104.041723.

Innan H, Kondrashov F. 2010. The evolution of gene duplications: classifying and distinguishing between models. *Nature Reviews Genetics* **11**:97–108 DOI 10.1038/nrg2689.

Ishikawa F, Suga S, Uemura T, Sato MH, Maeshima M. 2005. Novel type aquaporin SIPs are mainly localized to the er membrane and show cell-specific expression in *Arabidopsis thaliana*. *FEBS Letters* **579**:5814–5820 DOI 10.1016/j.febslet.2005.09.076.

Jang JY, Kim DG, Kim YO, Kim JS, Kang H. 2004. An expression analysis of a gene family encoding plasma membrane aquaporins in response to abiotic stresses in *Arabidopsis thaliana*. *Plant Molecular Biology* **54**:713–725 DOI 10.1023/b:plan.0000040900.61345.a6.

Javot H, Maurel C. 2002. The role of aquaporins in root water uptake. *Annals of Botany* **90**:301–313 DOI 10.1093/aob/mcf199.

Johanson U, Karlsson M, Johansson I, Gustavsson S, Sjövall S, Fraysse L, Weig AR, Kjellbom P. 2001. The complete set of genes encoding major intrinsic proteins in *Arabidopsis* provides a framework for a new nomenclature for major intrinsic proteins in plants. *Plant Physiology* **126**:1358–1369 DOI 10.1104/pp.126.4.1358.

Kadam S, Abril A, Dhanapal AP, Koester RP, Vermerris W, Jose S, Fritschi FB. 2017. Characterization and regulation of aquaporin genes of sorghum [*Sorghum bicolor* (L.) Moench] in response to waterlogging stress. *Frontiers in Plant Science* **8**:Article 862 DOI 10.3389/fpls.2017.00862.

Katsuhara M, Hanba YT, Shiratake K, Maeshima M. 2008. Expanding roles of plant aquaporins in plasma membranes and cell organelles. *Functional Plant Biology* **35**:1–14 DOI 10.1071/FP07130.

Koch MA, German DA. 2013. Taxonomy and systematics are key to biological information: *Arabidopsis*, *Eutrema* (*Thellungiella*), *Noccaea* and *Schrenkiella* (Brassicaceae) as examples. *Frontiers in Plant Science* **4**:Article 267 DOI 10.3389/fpls.2013.00267.

Kong W, Yang S, Wang Y, Bendahmane M, Fu X. 2017. Genome-wide identification and characterization of aquaporin gene family in *Beta vulgaris*. *PeerJ* **5**:e3747 DOI 10.7717/peerj.3747.

Leitão L, Prista C, Moura TF, Loureiro-Dias MC, Soveral G. 2012. Grapevine aquaporins: gating of a tonoplast intrinsic protein (TIP2;1) by cytosolic pH. *PLOS ONE* **7**:e33219 DOI 10.1371/journal.pone.0033219.

Li GW, Peng YH, Yu X, Zhang MH, Cai WM, Sun WN, Su WA. 2008. Transport functions and expression analysis of vacuolar membrane aquaporins in response to various stresses in rice. *Journal of Plant Physiology* **165**:1879–1888 DOI 10.1016/j.jplph.2008.05.002.

Li W, Qiang XJ, Han XR, Jiang LL, Zhang SH, Han J, He R, Cheng XG. 2018. Ectopic expression of a *Thellungiella salsuginea* aquaporin gene, TsPIP1;1, increased the salt tolerance of Rice. *International Journal of Molecular Science* **19**:Article 2229 DOI 10.3390/ijms19082229.

Li L, Wang H, Gago J, Cui H, Qian Z, Kodama N, Ji H, Tian S, Shen D, Chen Y, Sun F, Xia Z, Ye Q, Sun W, Flexas J, Dong H. 2015. Harpin hpa1 interacts with aquaporin PIP1;4 to promote the substrate transport and photosynthesis in *Arabidopsis*. *Scientific Reports* **5**:Article 17207 DOI 10.1038/srep17207.

Li X, Wang X, Yang Y, Li R, He Q, Fang X, Luu DT, Maurel C, Lin J. 2011. Single-molecule analysis of PIP2;1 dynamics and partitioning reveals, multiple modes of *Arabidopsis* plasma membrane aquaporin regulation. *The Plant Cell* **23**:3780–3797 DOI 10.1105/tpc.111.091454.

Liu C, Fukumoto T, Matsumoto T, Gena P, Frascaria D, Kaneko T, Katsuhara M, Zhong S, Sun X, Zhu Y, Iwasaki I, Ding X, Calamita G, Kitagawa Y. 2013. Aquaporin OsPIP1;1 promotes rice salt resistance and seed germination. *Plant Physiology and Biochemistry* **63**:151–158 DOI 10.1016/j.plaphy.2012.11.018.

Loqué D, Ludewig U, Yuan L, Wiren NV. 2005. Tonoplast intrinsic proteins AtTIP2;1 and AtTIP2;3 facilitate NH_3 transport into the vacuole. *Plant Physiology* **137**:671–680 DOI 10.1104/pp.104.051268.

Ma JF, Tamai K, Yamaji N, Mitani N, Konishi S, Katsuhara M, Ishiguro M, Murata Y, Yano M. 2006. A silicon transporter in rice. *Nature* **440**:688–691 DOI 10.1038/nature04590.

Ma S, Quist TM, Ulanov A, Joly R, Bohnert HJ. 2004. Loss of TIP1;1 aquaporin in Arabidopsis leads to cell and plant death. *The Plant Journal* **40**:845–859 DOI 10.1111/j.1365-313X.2004.02265.x.

Mao Z, Sun W. 2015. *Arabidopsis* seed-specific vacuolar aquaporins are involved in maintaining seed longevity under the control of abscisic acid insensitive 3. *Journal of Experimental Botany* **66**:4781–4794 DOI 10.1093/jxb/erv244.

Maurel C, Boursiac Y, Luu DT, Santoni V, Shahzad Z, Verdoucq L. 2015. Aquaporins in plants. *Physiological Reviews* **95**:1321–1358 DOI 10.1152/physrev.00008.2015.

Mitani-Ueno N, Yamaji N, Zhao FJ, Ma JF. 2011. The aromatic/arginine selectivity filter of NIP aquaporins plays a critical role in substrate selectivity for silicon, boron, and arsenic. *Journal of Experimental Botany* **62**:4391–4398 DOI 10.1093/jxb/err158.

Mizutani M, Watanabe S, Nakagawa T, Maeshima M. 2006. Aquaporin NIP2;1 is mainly localized to the ER membrane and shows root-specific accumulation in *Arabidopsis thaliana*. *Plant and Cell Physiology* **47**:1420–1426 DOI 10.1093/pcp/pcl004.

Park W, Scheffler BE, Bauer PJ, Campbell BT. 2010. Identification of the family of aquaporin genes and their expression in upland cotton (*Gossypium hirsutum* L.). *BMC Plant Biology* **10**:142 DOI 10.1186/1471-2229-10-142.

Putpeerawit P, Sojikul P, Thitamadee S, Narangaiavana J. 2017. Genome-wide analysis of aquaporin gene family and their responses to water-deficit stress conditions in cassava. *Plant Physiology and Biochemistry* **121**:118–127 DOI 10.1016/j.plaphy.2017.10.025.

Quigley F, Rosenberg JM, Shacharhill Y, Bohnert HJ. 2001. From genome to function: the *Arabidopsis* aquaporins. *Genome Biology* **3**:1–17 DOI 10.1186/gb-2001-3-1-research0001.

Reddy PS, Rao TSRB, Sharma KK, Vadez V. 2015. Genome-wide identification and characterization of the aquaporin gene family in *Sorghum bicolor* (L.). *Plant Gene* **1**:18–28 DOI 10.1016/j.plgene.2014.12.002.

Reuscher S, Akiyama M, Mori C, Aoki K, Shibata D, Shiratake K. 2013. Genome-wide identification and expression analysis of aquaporins in tomato. *PLOS ONE* **8**:e79052 DOI 10.1371/journal.pone.0079052.

Sakurai J, Ishikawa F, Yamaguchi T, Uemura M, Maeshima M. 2005. Identification of 33 rice aquaporin genes and analysis of their expression and function. *Plant Cell Physiology* **46**:1568–1577 DOI 10.1093/pcp/pci172.

Shivaraj SM, Deshmukh RK, Rai R, Bélanger R, Agrawal PK, Dash PK. 2017. Genome-wide identification, characterization, and expression profile of aquaporin gene family in flax (*Linum usitatissimum*). *Scientific Reports* **7**:46137 DOI 10.1038/srep46137.

Soto G, Fox R, Ayub N, Alleva K, Muschietti J. 2010. TIP5;1 is an aquaporin specifically targeted to pollen mitochondria and is probably involved in nitrogen remobilization in *Arabidopsis thaliana*. *The Plant Journal* **64**:1038–1047 DOI 10.1111/j.1365-313X.2010.04395.x.

Sreedharan S, Shekhawat UKS, Ganapathi TR. 2013. Transgenic banana plants overexpressing a native plasma membrane aquaporin MusaPIP1;2 display high tolerance levels to different abiotic stresses. *Plant Biotechnology Journal* **11**:942–952 DOI 10.1111/pbi.12086.

Sreedharan S, Shekhawat UKS, Ganapathi TR. 2015. Constitutive and stress-inducible overexpression of a native aquaporin gene (MusaPIP2;6) in transgenic banana plants signals its pivotal role in salt tolerance. *Plant Molecular Biology* **88**:41–52 DOI 10.1007/s11103-015-0305-2.

Sun HY, Li LC, Lou YF, Zhao HS, Gao ZM. 2016. Genome-wide identification and characterization of aquaporin gene family in moso bamboo (*Phyllostachys edulis*). *Molecular Biology Report* **43**:437–450 DOI 10.1007/s11033-016-3973-3.

Sun LL, Yu GH, Han XR, Xin SC, Qiang XJ, Jiang LL, Zhang SH, Cheng XG. 2015. TsMIP6 enhances the tolerance of transgenic rice to salt stress and interacts with target proteins. *Journal of Plant Biology* **58**:285–292 DOI 10.1007/s12374-015-0069-x.

Taji T, Seki M, Satou M, Sakurai T, Kobayashi M, Kanako I, Narusaka Y, Narusaka M, Tajkhorshid E, Nollert P, Jensen MØ, Miercke LJ, O'Connell J, Stroud RM, Schulten K. 2002. Control of the selectivity of the aquaporin water channel family by global orientational tuning. *Science* **296**:525–530 DOI 10.1126/science.1067778.

Takano J, Wada M, Ludewig U, Schaaf G, Von Wiren N, Fujiwara T. 2006. The *Arabidopsis* major intrinsic protein NIP5;1 is essential for efficient boron uptake and plant development under boron limitation. *The Plant Cell* **18**:1498–1509 DOI 10.1105/tpc.106.041640.

Tamura K, Stecher G, Peterson D, Filipski A, Kumar S. 2013. MEGA6: molecular evolutionary genetics analysis version 6.0. *Molecular Biology and Evolution* **30**:2725–2729 DOI 10.1093/molbev/mst197.

Tanaka M, Wallace IS, Takano J, Roberts DM, Fujiwara T. 2008. NIP6;1 is a boric acid channel for preferential transport of boron to growing shoot tissues in *Arabidopsis*. *The Plant Cell* **20**:2860–2875 DOI 10.1105/tpc.108.058628.

Tao P, Zhong X, Li B, Wang W, Yue Z, Lei J, Guo W, Huang X. 2014. Genome-wide identification and characterization of aquaporin genes (AQPs) in Chinese cabbage (*Brassica rapa* ssp. pekinensis). *Molecular Genetics and Genomics* **289**:1131–1145 DOI 10.1007/s00438-014-0874-9.

Uehlein N, Lovisolo C, Siefritz F, Kaldenhoff R. 2003. The tobacco aquaporin NtAQP1 is a membrane CO_2 pore with physiological functions. *Nature* **425**:734–737 DOI 10.1038/nature02027.

Venkatesh J, Yu JW, Park SW. 2013. Genome-wide analysis and expression profiling of the *Solanum tuberosum* aquaporins. *Plant Physiology & Biochemistry* **73**:392–404 DOI 10.1016/j.plaphy.2013.10.025.

Wang LL, Chen AP, Zhong NQ, Liu N, Wu XM, Wang F, Yang CL, Romero MF, Xia GX. 2014. The *Thellungiella salsuginea* tonoplast aquaporin TsTIP1;2 functions in protection against multiple abiotic stresses. *Plant & Cell Physiology* **55**:148–161 DOI 10.1093/pcp/pct166.

Wang Y, Li R, Li D, Jia X, Zhou D, Li J, Lyi SM, Hou S, Huang Y, Kochian LV, Liu J. 2017. NIP1;2 is a plasma membrane-localized transporter mediating aluminum uptake, translocation, and tolerance in Arabidopsis. *Proceedings of the National Academy of Sciences of the United States of America* **114**:5047 DOI 10.1073/pnas.1618557114.

Wu HJ, Zhang Z, Wang JY, Oh DH, Dassanayake M, Liu B, Huang Q, Sun HX, Xia R, Wu Y, Wang YN, Yang Z, Liu Y, Zhang W, Zhang H, Chu J, Yan C, Fang S, Zhang J, Wang Y, Zhang F, Wang G, Lee SY, Cheeseman JM, Yang B, Li B, Min J, Yang L, Wang J, Chu C, Chen SY, Bohnert HJ, Zhu JK, Wang XJ, Xie Q. 2012. Insights into salt tolerance from the genome of *Thellungiella salsuginea*. *Proceedings of the National Academy of Sciences of the United States of America* **109**:12219–12224 DOI 10.1073/pnas.1209954109.

Xu GX, Guo CC, Shan HY, Kong HZ. 2012. Divergence of duplicate genes in exon-intron structure. *Proceedings of the National Academy of Sciences* **109**:1187–1192 DOI 10.1073/pnas.1109047109.

Xu Y, Hu W, Liu J, Zhang J, Jia C, Miao H, Xu B, Jin Z. 2014. A banana aquaporin gene, MaPIP1;1 is involved in tolerance to drought and salt stresses. *BMC Plant Biology* **14**:59 DOI 10.1186/1471-2229-14-59.

Yang R, Jarvis DE, Chen H, Beilstein MA, Grimwood J, Jenkins J, Shu S, Prochnik S, Xin M, Ma C, Schmutz J, Wing RA, Mitchell-Olds T, Schumaker KS, Wang X. 2013. The reference genome of the halophytic plant *Eutrema salsugineum*. *Frontiers of Plant Science* **4**:Article 46 DOI 10.3389/fpls.2013.00046.

Yuan D, Li W, Hua YP, King GJ, Xu FS, Shi L. 2017. Genome-wide identification and characterization of the aquaporin gene family and transcriptional responses to boron deficiency in *Brassica napus*. *Frontiers of Plant Science* **8**:Article 1336 DOI 10.3389/fpls.2017.01336.

Zelazny E, Miecielica U, Borst JW, Hemminga MA, Chaumont F. 2009. An N-terminal diacidic motif is required for the trafficking of maize aquaporins ZmPIP2;4 and ZmPIP2;5 to the plasma membrane. *The Plant Journal* **57**:346–355 DOI 10.1111/j.1365-313x.2008.03691.x.

Zhang RB, Verkman AS. 1991. Water and urea permeability properties of Xenopus oocytes: expression of mRNA from toad urinary bladder.. *American Journal of Physiology* **260**:C26–C34 DOI 10.1152/ajpcell.1991.260.1.C26.

Zhang DY, Ali Z, Wang CB, Xu L, Yi JX, Xu ZL, Liu XQ, He XL, Huang YH, Khan IA, Trethowan RM, Ma HX. 2013. Genome-wide sequence characterization and expression analysis of major intrinsic proteins in soybean (*Glycine max* L.). *PLOS ONE* **8**:e56312 DOI 10.1371/journal.pone.0056312.

Zhu JK. 2001. Plant salt tolerance. *Trends in Plant Science* **6**:66–71 DOI 10.1016/S1360-1385(00)01838-0.

Zou Z, Gong J, Huang QX, Mo YY, Yang LF, Xie GS. 2015. Gene structures, evolution, classification and expression profiles of the aquaporin gene family in castor bean (*Ricinus communis* L.). *PLOS ONE* **10**:e0141022 DOI 10.1371/journal.pone.0141022.

Zou Z, Yang L, Gong J, Mo Y, Wang J, Cao J, An F, Xie G. 2016. Genome-wide identification of *Jatropha curcas* aquaporin genes and the comparative analysis provides insights into the gene family expansion and evolution in *Hevea brasiliensis*. *Frontiers of Plant Science* **7**:395 DOI 10.3389/fpls.2016.00395.